Chapter 13

Structure and Properties of the Multicomponent and Nanostructural Coatings on the Sintered Tool Materials

Leszek A. Dobrzański, Daniel Pakuła,
Klaudiusz Gołombek,
Anna D. Dobrzańska-Danikiewicz and
Marcin Staszuk

Additional information is available at the end of the chapter

http://dx.doi.org/10.5772/65400

Abstract

This chapter presents a general characteristic of sintered tool materials, in particular sintered sialons, nitride ceramics, injection-moulded ceramic-metallic tool materials and cemented carbides and a general characteristic of their surface treatment technology and especially chemical vapour deposition (CVD) and physical vapour deposition (PVD) techniques. The results of our investigations in technology foresight methods concerning the development prospects of surface engineering of sintered tool materials are presented. In the next subsection, we discuss the outcomes of multifaceted research carried out with advanced materials engineering methods, including high-resolution transmission electron microscopy, into the structure and properties of multicomponent, graded and multilayer coatings on the investigated tool materials, including the newly developed injection moulded ceramic-metallic tool materials. Special attention was drawn to a one-dimensional structure of the studied PVD and CVD coatings and its impact on the properties of coatings.

Keywords: sintered tool materials, foresight, surface engineering, PVD, CVD, coatings, nanostructure

1. General characteristic of sintered tool materials

Powder metallurgy has found widespread applications in the manufacture of sintered tool materials. Rapidly evolving techniques and technologies necessitate higher demands for sintered tool materials in terms of mechanical properties, among others wear resistance. Advanced sintered tool materials are witnessing constant advancements connected with fast

progress in materials engineering. Advanced sintered tool materials, due to the character of their work and complex wear mechanisms to which cutting tool edges are subjected, should satisfy numerous requirements including, in particular, high hardness, high impact strength, resistance to complex wear (adhesive, diffusive, abrasive and thermal wear) and to high temperatures, high compressive strength, stretching, flexing and bending, high fatigue and thermal strength, good conductivity and thermal capacity, cutting edge stability and good ductility [1–8]. A tool material with universal applications should merge the mentioned properties as far as possible and especially the highest wear resistance and hardness with high strength and good ductility accompanied by chemical inertness towards the workpiece. Despite the intensive development of materials engineering, a tool material has still not been produced which fulfil such requirements due to a fundamental contradiction between such properties as hardness and ductility.

As mentioned in the Introduction section, in general—in the group of sintered tool materials—one can distinguish super hard sintered materials, mixed ceramic and carbide materials, ceramic materials, steels and cermetals, including sintered high speed steels, sintered carbide steels and sintered carbides as well as injection moulded ceramic-metallic tool materials. The properties and intended use of the finished products made of sintered tool materials depend on the phase composition and a content of hard phase particles in sintered tool materials (whether they are present or not) and the chemical composition of a binding material, as well as the material's thermal workability.

Sialon ceramics known as sialon (the name comes from the first letters of the elements it contains, i.e. silicon, aluminium and oxy-nitride) was developed and introduced into production and application in industrial processes by the end of the twentieth century, as a new type of machining materials combining the advantages of oxide and oxide-free materials containing Si_3N_4 [2, 3]. Sialon, with its chemical composition determined by the formula $Si_{6-z}O_zN_{8-z}$, is isomorphic with silicon nitride Si_3N_4 (**Figure 1**). The number z = 0–4, 5 corresponds to the number of Al atoms replacing Si in the lattice of β nitride. Due to isomorphicity, the mechanical and physical properties of sialon β' are similar to the corresponding properties of Si_3N_4. The chemical properties of this phase correspond to aluminium Al_2O_3, though, sialon ceramics

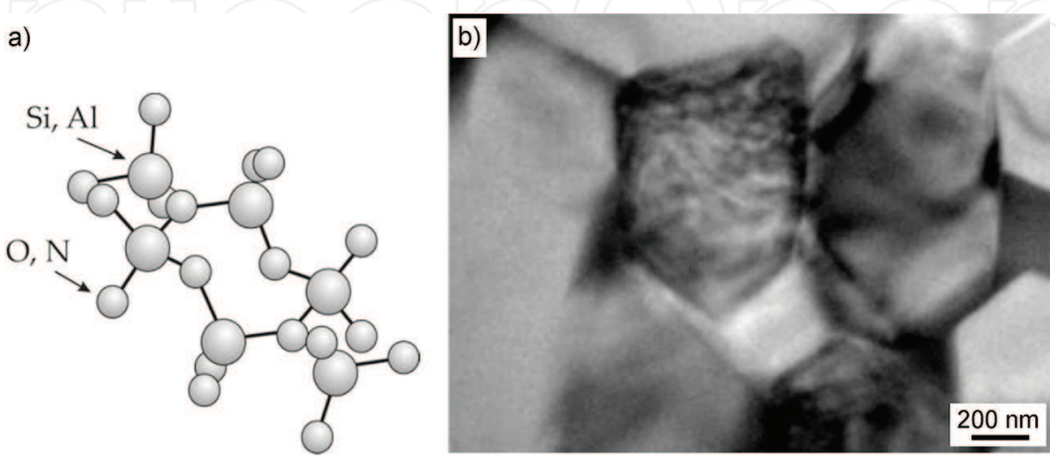

Figure 1. (a) Distribution of Si, Al, N and O atoms in crystallographic lattice of sialon β; (b) structure of thin foil parallel to the surface of sialon tool ceramics (TEM).

combines high physical and mechanical properties inherited from Si_3N_4 ceramics and resistance to chemical activity at a high temperature characteristic for Al_2O_3. Up to 60% of Al_2O_3 dissolves in sialon β', maintaining the hexagonal structure β-Si_3N_4. Sialons are most often produced using the method of one-stage reaction sintering of a moulded mixture of silicon nitride with an addition of oxide and aluminium nitride and a sintering additive, usually Y_2O_3, which is a source of the liquid phase during sintering. Very pure and fine-grained silicon nitride has to be utilised in this method.

Chemical composition has to be controlled very accurately during the process, as well, because even a small excess of oxygen increases the fraction of the liquid phase in sintering [3, 9]. It is favourable for technological reasons to introduce β' additives of other oxides, e.g. Y_2O_3, to a sialon sinter as this reduces vapour pressure and is essential for lowering a melting point of sialon β'. Pressure sintering instead of hot sintering is then feasible. In such case, a relatively low sintering temperature enables to maintain a fine-grained structure and thus to enhance the strength properties of the sinter. This also has an effect on a reduction in oxidisation resistance and supports accelerated decomposition of a solid solution at high temperatures. Glass is formed during cooling from a fluid created in intermolecular spaces during sialon β' densification with Y_2O_3 additive at high temperature. When heat treatment of such sinter is carried out again at 1400°C, the reaction of this glass with the β' sialon matrix takes place again:

$$\underset{\text{sialon } \beta'}{Si_5AlON_7} + \underset{\text{glass}}{Y\text{–}Si\text{–}Al\text{–}O\text{–}N} \rightarrow \underset{\text{sialon } \beta'}{Si_{5+x}Al_{1-x}N_{7+x}} + \underset{\text{YAG}}{Y_3Al_5O_{12}} \tag{1}$$

as a result of which a compound, $Y_3Al_5O_{12}$, called yttrium-aluminium-garnet (YAG), is created at the grain boundaries. The presence of this compound very effectively improves the resistance of sialon β' to oxidisation and creeping resistance.

Si_3N_4 nitride ceramics, due to its high thermomechanical properties, such as resistance to high temperature, low thermal expansion coefficient and high resistance to sudden temperature and chemical environmental changes, is regarded to be one of the most promising materials used in high-temperature processes. They exhibit high resistance to the activity of acids and reducing substances. Tools made of silicon nitride can work at the temperature of approximately 1400°C and maintain their mechanical properties. They are also resistant to corrosion and abrasion and receive thermal shocks very well. Nitride tool ceramics is manufactured by means of powder metallurgy and it is not necessary to melt the main component in a manufacturing process. This process is classical and, therefore, five main stages can be distinguished [3, 10], i.e. fabrication, preparation of powder, forming of preforms, sintering and finishing.

Si_3N_4 undergoes partial dissociation during heating above 750°C and sublimation at 2170°C. For this reason, a sintering process of silicon nitride at 1800–1900°C is conducted in glass or metallic capsules in the atmosphere of nitrogen. Sintered Si_3N_4 tool ceramics is obtained by uniaxial pressing or by hot isostatic pressing (HIP) and reactive sintering. The HIP sintering method consists of placing the sintered Si_3N_4 mass in a vacuum capsule and subjecting it to isostatic hot pressing. The simultaneous forming, sintering and compression take place; therefore, this method ensures relatively high bending strength and theoretical sinter density [11, 12].

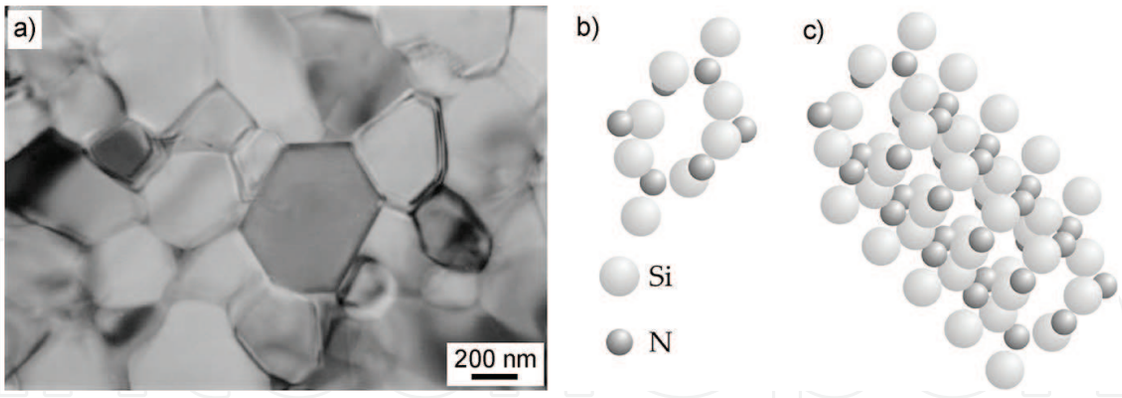

Figure 2. Structure of (a) thin foil parallel to the surface of tool layer of nitride Si_3N_4 ceramics (TEM); crystalline β-Si_3N_4 (b) single unit cell, (c) six unit cells.

Pure Si_3N_4 exhibits high strength, hardness and oxidisation resistance. After adding the necessary densifiers during sintering, i.e. MgO, Y_2O_3, Al_2O_3, HfO_2 or TiC, the very good properties deteriorate. Silicon nitride is susceptible to a chemical interaction of the treated material and to oxidisation during work at the temperature of 1000–1200°C. The properties of nitride ceramics are further improved by introducing additives in the form of zirconium oxide (ZrO_2), titanium nitride (TiN) or SiC whiskers [13]. Hardness, plasticity and wear resistance are then increased. Nitride tool ceramics exhibits a β crystalline structure after sintering (**Figure 2**) [12, 14]. Si_3N_4 nitride may be used with the addition of Y_2O_3 or TiC particles, dispersive in 30%, can be placed in a matrix containing 92% of Si_3N_4, 6% of Y_2O_3 and 2% of Al_2O_3.

The injection moulded ceramic-metallic tool materials described in this chapter were manufactured in laboratory conditions at a quarter-technical scale. Nevertheless, it was decided to incorporate them due to the expected high development prospects of this manufacturing method and of this group of ceramic-metallic materials. This technology enables to produce relatively small elements with complicated shapes and a developed surface, which in turn is a significant limitation in the application of classical powder metallurgy. The assumptions of this method are described in one of the preceding chapters. In the powder injection moulding (PIM)

	Mixture composition, %								Content of components, %		
Designation	**WC**	**TiC**	**TaC**	**NbC**	**VC**	**Co**	**Ni**	**Designation**	**Polypropylene**	**Paraffin**	**Stearic acid**
TC	33	33	25	8	–	1	–	TC60SA4	18	18	4
								WS!60SA4	18	18	4
WS1	57	20	14		–	9	–	WS157SA2	20.5	20.5	2
								WS154	23	23	0
WS2	87	5	–	–	–	8	–	WS260SA4	18	18	4
								WS260SA4	18	18	4
WS3	69	20			2	5	4	WS354SA4	21	21	4
								WS360SA4	18	18	4

Table 1. Characteristic of mixtures of powders and components of a binder of newly developed ceramic-metallic tool materials by the PIM method.

http://dx.doi.org/10.5772/65400

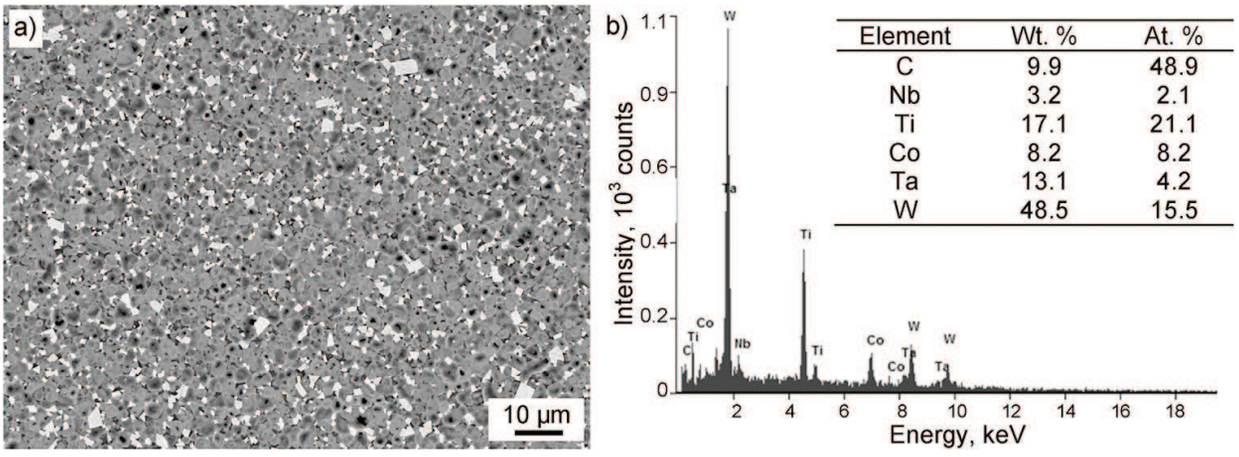

Element	Wt. %	At. %
C	9.9	48.9
Nb	3.2	2.1
Ti	17.1	21.1
Co	8.2	8.2
Ta	13.1	4.2
W	48.5	15.5

Figure 3. Substrate structure of WS1 tool material (a); EDS spectrum from area as in figure (a) and results of quantitative analysis of chemical composition (b).

method [2, 6–8, 15–25], a mixture of polymer (binder) and powders of inorganic materials is supplied to a cylinder equipped with a worm screw which, when rotating, is moving the heated mixture until the required volume of the fed material is achieved and a polymer-powder slip is sprayed into a moulding die. A brittle preform is subjected to further heating at a small rate and to long annealing for full or partial decarbonisation and then to sintering. Despite its relatively low 4% share in the global market of products manufactured with the PIM technology, the fabrication of advanced tool materials by this method has received considerable interest [2, 3, 15, 21], as it is a highly profitable technology and forms a basis for obtaining a broad group of universal tool materials that are highly complex, accurate, even considering complex geometrical features, in the form assumed, according to the requirements of the near-net-shape technology without performing finish treatment, e.g. grinding and sharpening before the deposition of coatings.

The mixtures of powders described in this work [5] were used for fabricating the newly established tool ceramic-metallic materials. Such mixtures are the key component of the charge (**Table 1**) together with slip agents (WS symbols) and were manufactured by Treibacher Industrie AG without a slipping agent (symbol: TC). A mixture of polypropylene and paraffin was used as a binder with some contents of stearic acid used as a surfactant (**Table 1**).

It was found as a result of observations in a scanning electron microscope that ceramic-metallic tool materials have a homogeneous structure with uniformly distributed hard melting carbides in a cobalt or nickel-cobalt matrix without visible precipitations of free graphite and an undesired phase η and without visible microporosity. The structure of composite tool materials of the WS1 and WS2 type is characterised by fine grains of carbides, with the size of 1–3 and 2–4 µm, respectively, arranged in a cobalt matrix. The size of carbide grains in a cobalt-nickel matrix in a WS3 tool material is 0.5–2 µm (**Figure 3**).

It was found based on the examinations of thin foils in an electron microscope that the structure of the investigated WS1 and WS2 tool materials consists of a solid solution of cobalt or cobalt and nickel γ filling the space between WC, TiC, TaC, NbC and VC carbide particles (**Figure 4**). It was also found that the average diameter of the major part of carbide particles is smaller than 2 nm, which clearly classifies the studied WS1 and WS3 carbides to the group of

fine-grained materials. It was also stated that numerous crystalline structure defects exist in the structure of hard melting carbides (**Figure 4c**).

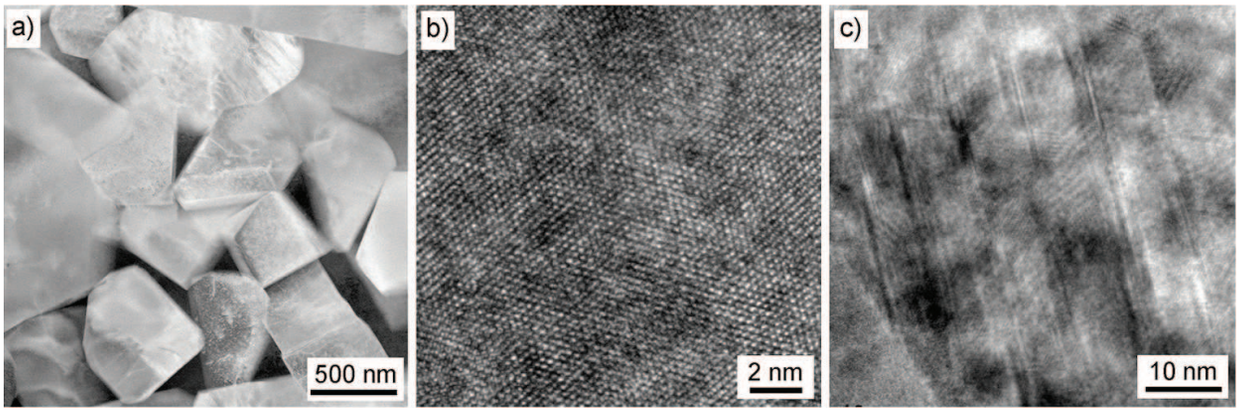

Figure 4. Structure of thin foil made from tool material (a) WS3, (b) & (c) WS1; (a) image in scanning-transmission mode, HAADF detector, (b) & (c) image in HRTEM mode.

The sintered carbides of metals are materials commonly used for cutting tools, manufactured by conventional powder metallurgy methods. Sintered carbides are materials consisting of carbides of hard melting metals, mainly W and also Ti, Ta and Nb, with a volume fraction of approximately 65–95% and a binding metal, usually cobalt. Sintered carbides can also be produced in which a binding metal is nickel, molybdenum and iron or their alloys with cobalt. The most often used types of sintered carbides include such used for the machining of materials producing a chipping, long—mainly steel and cast steel, both long and short, short—mainly cast iron, used for plastic working and for abrasion resistant device parts and also for reinforcement of mining tools. Such materials are also discussed in other chapters of the book. Carbide powders in the first stage of sintered carbides' production are usually fabricated by one of the three methods, i.e. multistage, shortened and single-stage method [2, 3, 8].

The shortened method is applied most often due to the highest efficiency and lowest costs. Sintering is usually done in induction or resistance vacuum furnaces. The single-stage method is used for special purposes—for manufacture of large products and products without pores and also for manufacture of products exposed in service to impact loads and products used for tools for plastic working. Additional densification during hot isostatic pressing at the temperature of 1350–1450°C under the argon pressure of 100–300 MPa has a decisive effect on the higher bending strength of sintered carbides and their higher density.

Sintered carbides' structure is shown in **Figure 5**. The following phases may exist in the structure of sintered carbides at room temperature [2, 3]:

- α—sintered particles initiating particles of tungsten carbide WC,
- α_1—solid secondary solution of cobalt in tungsten carbide WC, uncrystallised during sintering, existing in the form of fine-rounded grains,

http://dx.doi.org/10.5772/65400

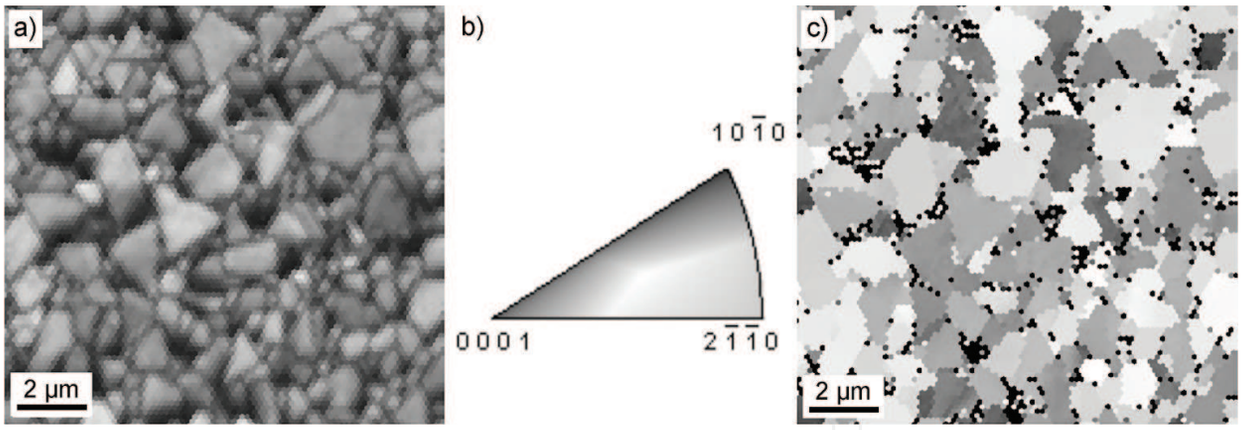

Figure 5. The results of analysis of sintered carbides WC-Co performed by diffraction of back scattered electrons (EBSD), (a) distribution map of diffraction quality, (b) reverse pole figures and (c) crystallographic orientation map of WC grains.

- α_2—solid secondary solution of cobalt in tungsten carbide WC, created as a result of crystallisation during sintering, existing as large grains with regular shapes,
- γ—solid solution of tungsten, tantalum and carbon in cobalt,
- β—(Ti,W)C, (Ta,W)C or (Ti,Ta,W)C carbides in the form of chains or ball grains,
- β'—phase β impoverished in tungsten with a higher concentration of titanium or tantalum.

The following phases can be formed in the case of insufficient carbon:

- η—a phase with a complex structure Co_3W_3C,
- Θ—a phase with a complex structure $Co_3W_6C_2$,
- χ—a phase with a complex structure $Co_3W_{10}C_4$,
- δ—Co_3W type phase.

Sintered carbides are not subjected to heat treatment as a binding metal is not subjected to phase transformations [2, 3]. Sintered carbides are not suitable for plastic and mechanical working, either, consisting of rolling and milling. They can be, however, polished or ground in or undergo surface treatment consisting of the deposition of abrasion resistance coatings.

2. General characteristic of surface treatment technologies of sintered tool materials

One of the development directions, undergoing the most intensive growth, of advanced tool materials, including sintered carbides, tool ceramics and tool cermetals, is the deposition of anti-wear coatings, usually nanostructured coatings, onto such materials, mainly in physical vapour deposition (PVD) and chemical vapour deposition (CVD). The possibilities of constituting coatings resulting from the interaction between the fabrication method, the properties

and the efficiency of the system produced allow, by matching them appropriately, to fabricate coatings possessing the expected functional properties [1–3].

The research topics concerning the fabrication of coatings with good mechanical properties and high abrasive wear resistance, including PVD and CVD, represent one of the most essential directions of surface engineering development [1–3, 26–30]. Enhanced operational properties are very frequently achieved for commonly applied materials by depositing simple monolayer, single-component coatings with PVD methods. When selecting a coating material, a constraint is encountered resulting from the fact that many properties expected from an ideal coating cannot be achieved at the same time. For instance, improved hardness and strength are reduced ductility and substrate adhesion of a coating. Coatings with different properties were bonded together for this reason, with each of them performing a relevant task aimed at achieving continuous or graded coatings with possibly most desired properties in a specific application. Graded coatings are deposited by changing gradually or continuously one or several components in the direction from the substrate to the outer surface. They represent a modern group of coatings achieved by PVD [1–3, 26, 29]. The layers or zones of the coating being produced should ensure, depending on their location, the desired properties and—by creating transition zones—guarantee transition between the properties that often vary. The layer closest to the material being coated generally ensures best adhesion to the substrate while the outer layer ensures adequate hardness, strength, tribological and anticorrosive properties. When coatings are fabricated in which chemical composition changes gradually from the substrate to the surface, it is possible to apply such coatings as anticorrosive coatings and also for structural parts, in particular for turbines and implants and surgical and dental implant-scaffolds [31–38].

A technological trend observed for many years in the field of tools production, not only cutting tools, is the deposition of anti-wear coatings onto tool materials, including those achieved by PVD and CVD and also with other advanced technologies. Numerous research studies in the recent years, including own studies [5, 26–30, 39–51], concerning deposition using coatings resistant to the wear of tool ceramics, have verified the existing stance that it is unsubstantiated to coat tool ceramics due to their high hardness. It has been demonstrated that it is clearly reasonable to coat such tools as, first of all, the life of tools' cutting edges is enhanced by decreasing the heat emitted while cutting, by reducing a friction force on the flank surface and, secondly, it was noted that coatings, by covering pores on the surface of tool ceramics, eliminate places where fractures occur and moreover, they delay the diffusion wear process. By resolving such a research problem, it is also possible to improve the efficiency and quality of machining, while reducing its energy consumption and material consumption, which is a prerequisite for ensuring competition in the conditions of free market economy. If the surface machining technology of tool materials is employed, including PVD and CVD methods, to attain graded layers with high wear resistance, also at high temperatures, the properties of such materials in machining conditions can be enhanced, among others by lowering the friction factor, ameliorating microhardness, improving conditions of tribological contact within the contact area of the tool-workpiece; adhesion and diffusion wear and oxidisation can also be prevented. If such properties are found, an optimum field of applications can identified for the ceramic materials of a substrate and for the studied multiphase and graded

layers. Furthermore, a correlation can be determined between the results of laboratory investigations and the wear identified as a result of technological cutting tests.

3. Own investigations of development perspectives of surface engineering of sintered tool materials

Having regard to the main development directions aimed at the improvement of sintered tool materials, apart from searching completely new materials and improving the chemical composition of the existing materials, surface treatment should be mentioned to improve their properties [52–54]. Clients expect that advanced sintered tool materials should have a wide group of properties determining their functional characteristics, as mentioned in the above subsection. The purpose of advanced technologies for the formation of the structure and properties of surface tool materials is to reach the optimum combination of the expected properties for a specific material and a product made of it.

Scientific methods were applied in the framework of the own foresight research performed—which also utilised the production process optimisation methods—in order to determine the strategic development directions of technologies, the recognition and implementation of which is to contribute towards the greatest economic and social benefits of knowledge- and innovation-based economy [55, 56]. Over 500 detailed technologies of structure and surface properties formation of engineering materials were considered in the implemented project concerning the development trends of engineering materials and biomaterials, in which approximately 500 scientists from many countries of the world participated. All the analysed technologies were grouped into 14 thematic areas (*P*1–*P*7 and *M*1–*M*7) and 10 critical technologies—considered to be a priority with the best development prospects and/or of crucial importance for the industry over the next 20 years—were chosen for each of the selected areas. The considered thematic areas encompass four areas pertaining to the treatment technologies of sintered tool materials: (1) *P*4: surface engineering of tool materials; (2) *M*2: physical vapour deposition technologies (PVD); (3) *M*3: chemical vapour deposition technologies (CVD); (4) *M*6: technologies of nanostructural surface layers [52, 53].

The best critical technologies concerning the surface treatment of sintered tool materials were presented graphically with a technology strategy matrix (**Figure 6**). A universal scale of relative states consisting of 10 scores was used to evaluate individual technologies for their value and environment influence intensity. According to the scale, which is a single-pole positive scale without zero, the lowest possible score is 1 and the highest score is 10. A 16-field matrix of strategies for technologies, indicating a long-term procedure for a given technology, derives from a four-field dendrological matrix of technology value and a four-field meteorological matrix of environment influence [52].

The dendrological matrix presents graphically expert evaluation results of the individual technologies for their potential, representing an objective value of the given technology and their attractiveness, reflecting the subjective perception of the given technology by its potential users. The best quarter of the dendrological matrix is a *wide-stretching oak* to which technologies are

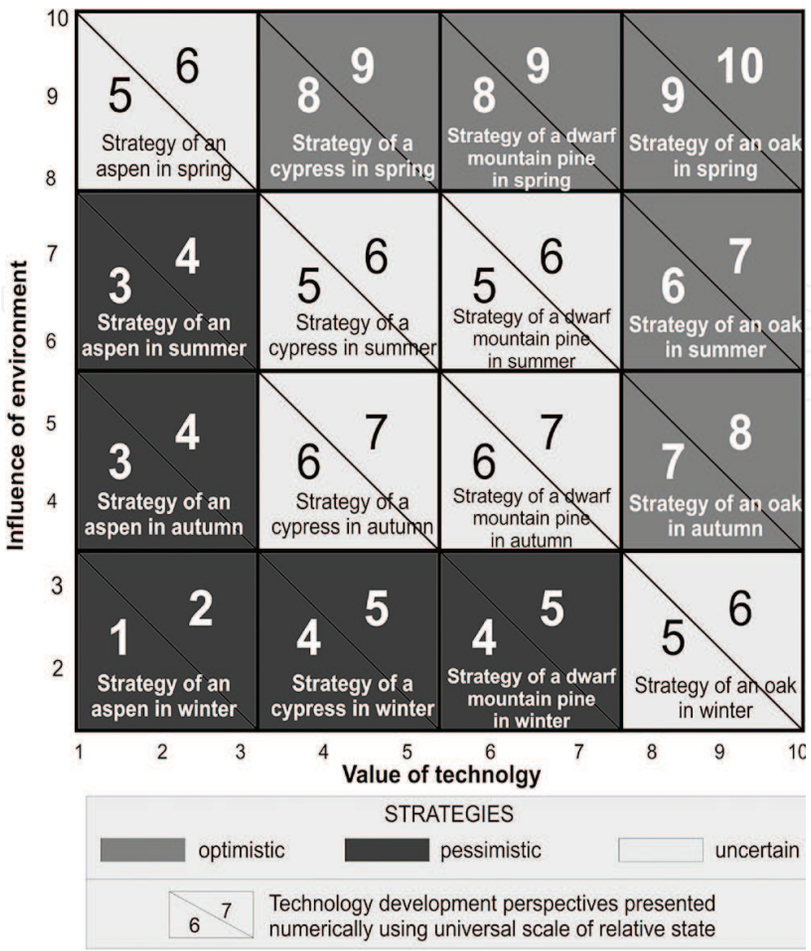

Figure 6. Matrix of strategies for technologies in general form.

assigned having high potential and attractiveness. If a technology is placed in a quarter *rooted dwarf mountain pine*, with a high potential and limited attractiveness, or in a quarter *soaring cypress*, with high attractiveness and limited potential, this means that a market success is possible in advantageous market conditions. A *quaking aspen* is a quarter with poor perspectives, though, to which technologies are assigned having a low potential and low attractiveness.

The meteorological matrix presents graphically the effect of positive and negative factors on the technologies, called opportunities and difficulties, respectively. In the best variant, called *sunny spring*, many positive stimuli come from the environment having influence on the technologies and difficulties are small. Peaceful and sustainable development of technologies is also possible as it is impacted by numerous positive and negative factors, which takes place when technologies are in the quarter *rainy autumn*. A quarter called *hot summer* corresponds to a risky environment bringing many opportunities and risks for technologies. The worst possible variant, in which many difficulties exist affecting the technologies adversely, accompanied by scarce opportunities, is called the quarter *frosty winter*.

An analysis carried out according to the results of foresight research, presented graphically using matrices called contextual matrices—due to graphical references to the commonly

http://dx.doi.org/10.5772/65400

known objects and phenomena—allowed to determine the strategic position of the critical technologies of surface engineering of sintered tool materials. The most promising technologies are presented in **Table 2**. They are characterised by high attractiveness and potential and environmental conditions are very helpful here, which is manifested by numerous opportunities and a small number of external difficulties. They are placed in the best 16 matrices of strategies for technologies called *oak in spring*, as shown in **Figure 7**. For such technologies, a

Surface engineering of tool materials *P*4	
A_{P4}	Physical vapour deposition (PVD)
B_{P4}	Chemical vapour deposition (CVD)
Physical vapour deposition technologies (PVD) *M*2	
A_{M2}	Cathodic arc deposition (CAD)
B_{M2}	Reactive magnetron sputtering (RMS)
Chemical vapour deposition technologies (CVD) *M*3	
D_{M3}	Plasma-assisted/enhanced chemical vapour deposition (PACVD/PECVD)
E_{M3}	Laser chemical vapour deposition (LCVD)
G_{M3}	Metal organic chemical vapour deposition (MOCVD)
Technologies of nanostructural surface layers *M*6	
D_{M6}	Ion beam-assisted deposition (IBAD)
E_{M6}	Electron beam physical vapour deposition (EB-PVD) of nanometric surface layer

Table 2. Key critical technologies of surface engineering of sintered tool materials.

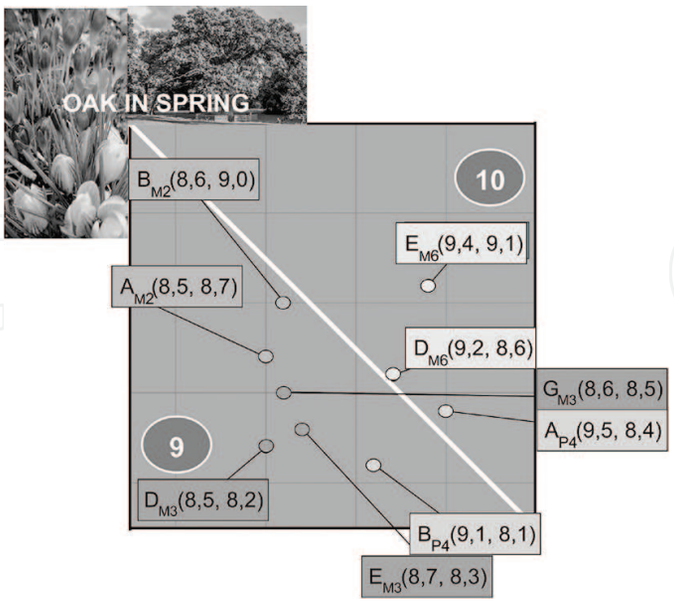

Figure 7. The best 16 matrices of strategies for technologies with points marked (top right corner), whose coordinates correspond to expert evaluation of key values of technologies and intensity of environment influence on such technologies.

winning strategy should be applied, consisting of developing, strengthening and implementing an attractive technology with a high potential in industrial practise while taking advantage of favourable environmental conditions in order to achieve a spectacular success.

The results of expert opinions presented in contextual matrices derive from the statistical surveys presented as a bar chart (**Figure 8**). As part of such heuristic research, the experts identified the forecast development trends of given technologies against the analysed thematic areas, by predicting whether the importance of particular groups of technologies in the nearest 20 years will be growing, maintaining at the same level or declining. In all the charts, grey bars correspond to, in per cents, the predicted growth of importance of a given technology group, light grey—stabilisation at the existing level and dark—a declining importance of the technology group against other technology groups of a given thematic area.

The presented results of foresight research indicate that PVD and CVD methods play a crucial role in the group of numerous surface treatment technologies applicable with respect to sintered tool materials. The most promising PVD methods include cathodic arc evaporation (CAD) and reactive magnetron sputtering (RMS). With respect to CVD methods, the best development prospects are seen for methods using plasma for assistance (PACVD/PECVD), metalorganic precursors (MOCVD) and laser (LCVD). If nanometric surface layers have to be deposited onto sintered tool materials, it is the experts' opinion that it is most advantageous to employ PVD methods with ion beam assisted deposition (IBAD) or electron beam physical vapour deposition (EB-PVD) [52–54]. The outcomes of the analyses performed may be a basis for studies aimed at the industrial implementation of the mentioned critical technologies, for

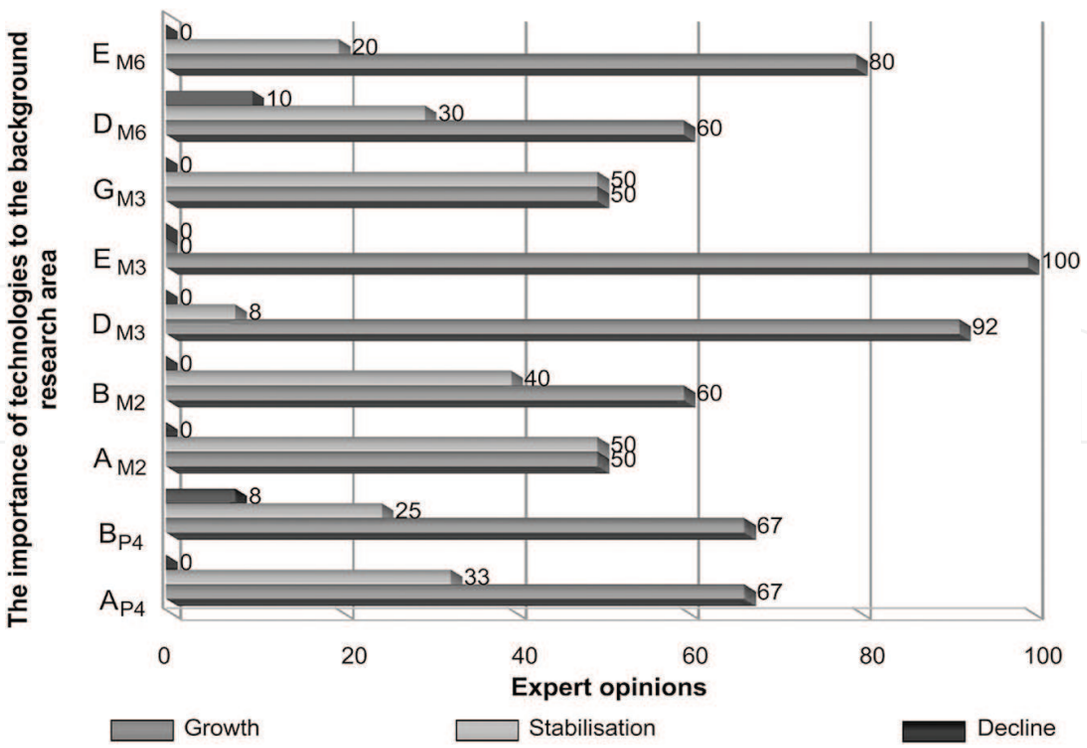

Figure 8. The predicted trends in changes of importance of key critical technologies of surface engineering of sintered tool materials.

example in production of cutting tools made of sintered materials, which undoubtedly provides an opportunity to improve the functional properties of the analysed group of tool materials.

4. Investigations into the structure of multicomponent coatings on the investigated sintered tool materials

The subchapter below is summarising and generalising the results of own investigations, pursued over the last decade, into the structure of sintered sialons, nitride ceramics, injection moulded ceramic-metallic tool materials and cemented carbides onto which wear resistant coatings are deposited. The methodology and detailed results of particular investigations of mechanical and functional properties of sintered tool materials with PVD and CVD coatings are presented in the own works published earlier [5, 26–30, 39–52]. The scientific aim of this paper is to present investigations into the structure and properties and to identify wear mechanisms for tools fabricated from the investigated sintered tool materials, which—to some extent—are newly created with newly developed nanocrystalline multiphase and graded coatings applied by PVD with cathodic arc evaporation techniques, as well as by a high-temperature CVD process, with the intention to improve the cutting properties of the investigated materials by considerably improving the life of the tool cutting edge. The state-of-the-art materials science research methods were employed for explaining the causes of a marked improvement in the operational properties of the tools, especially thin foils tests, including on cross sections in a high-voltage transmission electron microscope. Such coatings have not been applied to date onto any tools made of the materials mentioned. Investigations are known, however, concerning the deposition of similar coatings onto tools made of classical sintered carbides and cermetals. The deposition of coatings achieved in a CVD process onto nitride ceramics with a combination of Al_2O_3+TiN layers [28, 48, 51] is also known. The results of such research constitute a reference point for the results of the own research presented in this subchapter.

Indexable inserts made of sintered carbides and sialon and nitride tool ceramics were deposited in the process of cathodic arc evaporation (CAE-PVD) with graded coatings of the following type: Ti(B,N), (Ti,Zr)N, Ti(C,N), Ti(C,N)+(Ti,Al)N, TiN+(Ti,Al,Si)N+(Al,Si,Ti)N and the following multiphase coatings: (Al,Ti)N, (Ti,Al)N, (Al,Cr)N, (Ti,Al)N+(Al,Cr)N, (Al,Cr)N+(Ti, Al)N, TiN+multi(Ti,Al,Si)N +TiN, TiN+(Ti,Al,Si)N+TiN, as well as in a high-temperature CVD process with multilayer coatings based on Ti(C,N), Al_2O_3, TiN and TiC phases [1, 27–30, 41, 48–51]. The thickness of the investigated PVD coatings obtained in sintered carbides and tool ceramics spans between 0.7 and 5.0 μm, while the thickness of CVD coatings spans between 1.7 and 10 μm.

Note that 10 layer nanocrystalline surface coatings of the (Cr,Al,Si)N and (Al.Ti,Si)N types were applied alternatively by the modified lateral arc rotating cathodes (LARC) technique into a substrate made of the investigated ceramic-metallic tool materials [5]. CrN or TiN, respectively, were used as near-the-core layers, by placing them onto graded layers (Cr,Al)N/(Al,Cr)N and (Ti,Al)N/(Al,Ti)N, respectively. Note that eight multilayers were successively deposited

onto such layers with a variable composition in the following order: (Cr,Al,Si)N+(Al,Cr,Si)N +(Cr,Al,Si)N+(Al,Cr,Si)N+(Cr,Al,Si)N+(Al,Cr,Si)N+(Cr,Al,Si)N and, respectively, (Ti,Al,Si)N +(Al,Ti,Si)N+(Ti,Al,Si)N+(Al,Ti,Si)N+(Ti,Al,Si)N+(Al,Ti,Si)N +(Ti,Al,Si)N. The total thickness of CrAlSiN and AlTiSiN coatings is 2.5–3.0 μm. Regardless the location, all the layers forming part of the coatings tightly adhere to each other and do not show any fractures and discontinuities. In addition, fractographic tests of tool materials with the deposited (Cr,Al,Si)N and (Al,Ti,Si)N coatings do not reveal any delamination along the separation area between the coating and the substrate and show that the coatings obtained adhere strongly to the substrate.

A qualitative phase composition analysis carried out using the X-ray diffraction method confirms that coatings exist containing TiN, Ti(C,N), AlN and CrN phases and an Al_2O_3 phase in the case of CVD coatings on substrates made of sintered carbides and tool ceramics. The presence of isomorphic TiN phases was identified on the X-ray diffraction patterns obtained from Ti(B,N), (Ti,Zr)N, Ti(C,N)+(Ti,Al)N and (Ti,Al)N coatings because such phases are a secondary TiN-based solid solution. In the case of Ti(C,N) (1) and Ti(C,N) (2) coatings, the presence of titanium carbonitride was confirmed and in the case of (Al,Ti)N and (Al,Cr)N coatings, a diffraction analysis showed the presence of the AlN phase with a hexagonal lattice in the both coatings and of TiN and CrN phases, respectively. Moreover, the presence of reflexes from the substrate was determined in some cases, which is due to the fact that the thickness of the coatings is smaller than the penetration depth of X-ray beams inside the tested material.

The results of an X-ray qualitative phase analysis performed with Bragga-Brentano geometry of surface coatings of (Cr,Al,Si)N and (Al,Ti,Si)N type deposited onto ceramic-metallic tool materials (**Figure 9**) point out, as assumed, that coatings were produced on the surface of the investigated sintered carbides containing AlN and CrN phases. It is not possible to differentiate between AlN and (Al,Ti,Si)N, CrN and (Cr,Al,Si)N phases with diffraction methods because the phases are isomorphic, as, in fact, both (Al,Ti,Si)N and (Cr,Al,Si)N are secondary solid solutions based on chromium nitride CrN and aluminium nitride AlN, respectively.

It was found based on the analyses undertaken that a concentric intensity distribution of pole figures, varying along the axis of such figures, indicates the presence of a constituent axial texture

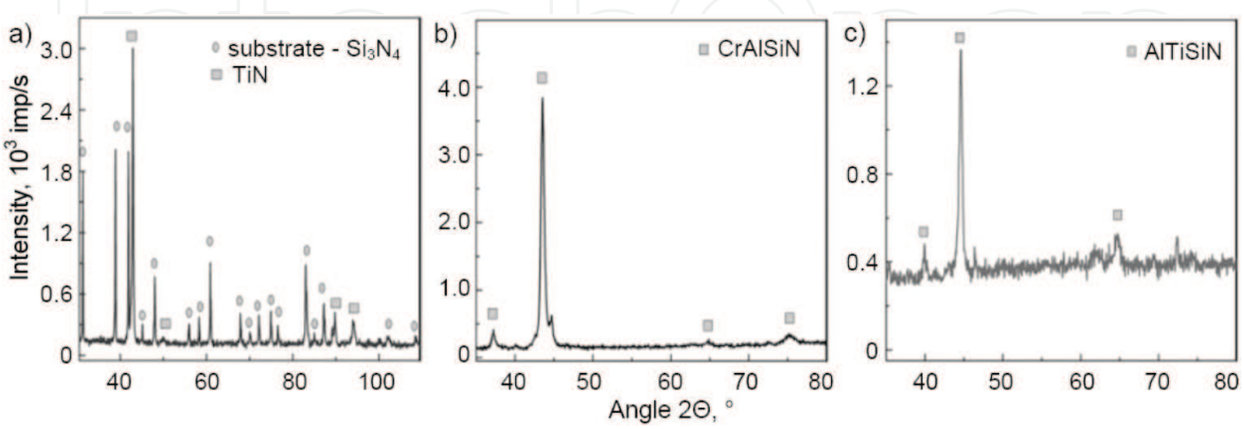

Figure 9. X-ray diffraction pattern of (a) Ti(B,N) coating deposited on the sialon ceramics, (b) CrN/(Cr,Al,Si)N coating and (c) AlN/(Al,Ti,Si)N coating deposited onto WS3 tool material, obtained by the Bragg-Brentano method.

of coatings produced with the cathodic arc evaporation technique on a substrate made of the investigated ceramic-metallic tool materials. Both, in the case of CrN/(Cr,Al,Si)N coatings and AlN/(Al,Ti,Si)N coatings, the intensity growth areas on the registered figures correspond to the double texture <200> and <311>, respectively, a quantitative fraction of the distinguished component <200> is 33 and 26% and of the component <311>–8.6 and 5.6% (**Figure 10**).

Variations in the atomic concentration of coating components in the direction perpendicular to the coating surface and concentration variations in the transition zone between the coating and the substrate material, depending on the number of layers deposited, were examined in a GDOS glow discharge optical spectrometer. The correct distribution of the elements forming part of the coatings and the substrate was determined. All the elements forming part of the investigated coatings occur only in the area of coatings and elements forming part of ceramics exist in the substrate area. The examinations confirm the existence of the relevant elements in the graded layers Ti(B,N), (Ti,Zr)N, Ti(C,N) (1), Ti(C,N) (2), (Al,Ti)N and in multilayer coatings Ti(C,N)+(Ti,Al)N, (Al,Cr)N+(Ti,Al)N, Ti(C,N)+Al_2O_3+TiN, Ti(C,N)+TiN (**Figure 11**). A curve of variations in a concentration of the elements forming the coatings shows their gradient structure.

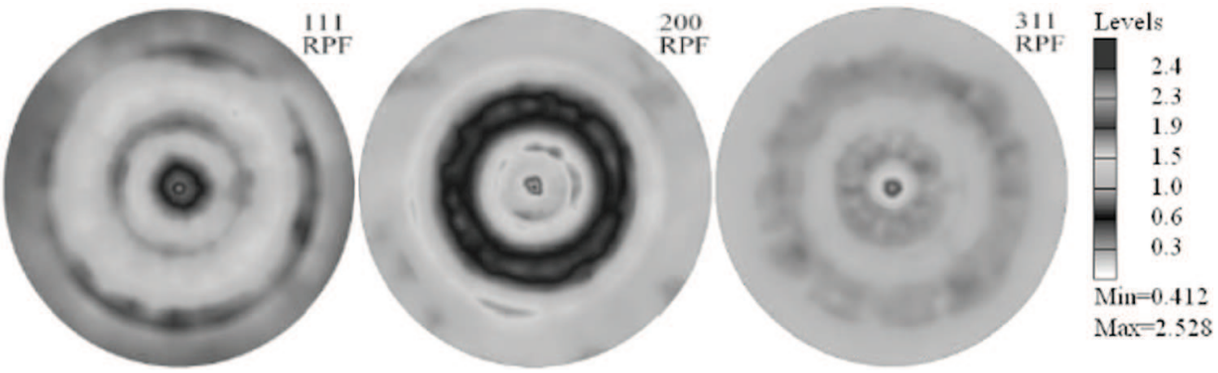

Figure 10. Pole figures (111), (200) and (311) of CrN/(Cr,Ti,Si)N coating on tool material WS1 calculated from FRO.

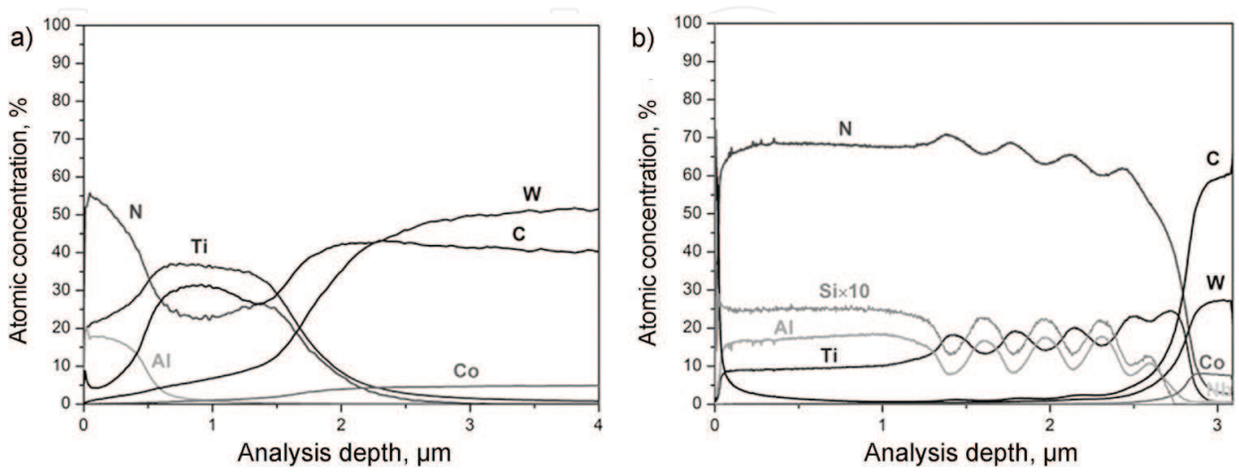

Figure 11. Changes analysed in the GDOS spectrometer of constituent concentration of (a) the Ti(C,N)+(Ti,Al)N coating on the sintered carbides substrate; (b) (Al,Ti,Si)N on WS1 ceramic-metallic tool material.

It was established through a GDOES analysis that a concentration of the elements forming part of the substrate is growing in a bonding zone from the surface of coatings with a reduction, at the same time, in a concentration of the elements forming part of the coating (**Figure 11**). This fact may be linked to the presence of a transition zone of a diffusive character between the substrate material and the coating, as suggested by the authors in earlier studies [1, 5, 57–59]. It cannot be precluded, however, that uneven evaporation of the material is possible at the same time from the surface of the specimens during an examination in a glow discharge spectrometer. The existence of a transition layer should be associated with the higher desorption of the substrate surface and with the formation of defects in a substrate as well as with the mixing of elements in a bonding zone due to the activity of high-energy ions. The existence of diffusive transition layers is supportive to the good adhesion of coatings to the substrate.

A profile analysis of chemical composition in the function of distance from the surface with the deposited (Cr,Al,Si)N and (Al,Ti,Si)N coatings on a substrate made of the investigated ceramic-metallic tool materials, as well as variations in a concentration of particular elements in a transition zone between such layers and a substrate material from the investigated ceramic-metallic tool materials were evaluated based on tests with a GDOS-850 glow discharge optical spectrometer (**Figure 12**). The character of variations in the substrate-coating bonding zone and between particular layers also confirms that transition layers exist here having the diffusive nature, as it was indicated earlier with respect to the other examined substrate materials.

An analysis of the chemical state of elements and of variations in a chemical concentration of components of (Cr,Al,Si)N and (Al,Ti,Si)N-type layers on a substrate made of the investigated ceramic-metallic tool materials was performed using the X-ray photoelectron spectroscopy (XPS) and auger electron spectroscopy (AES) technique (**Figure 12**). Photoelectric lines on an XPS spectrum obtained from a (Cr,Al,Si)N coating deposited onto a WS3 ceramic-metallic tool material, which are situated near the energy of 670.8 and 683.5 eV, derive from a 3d band of xenon atoms' electrons produced from the process of surface cleaning and are needed to create

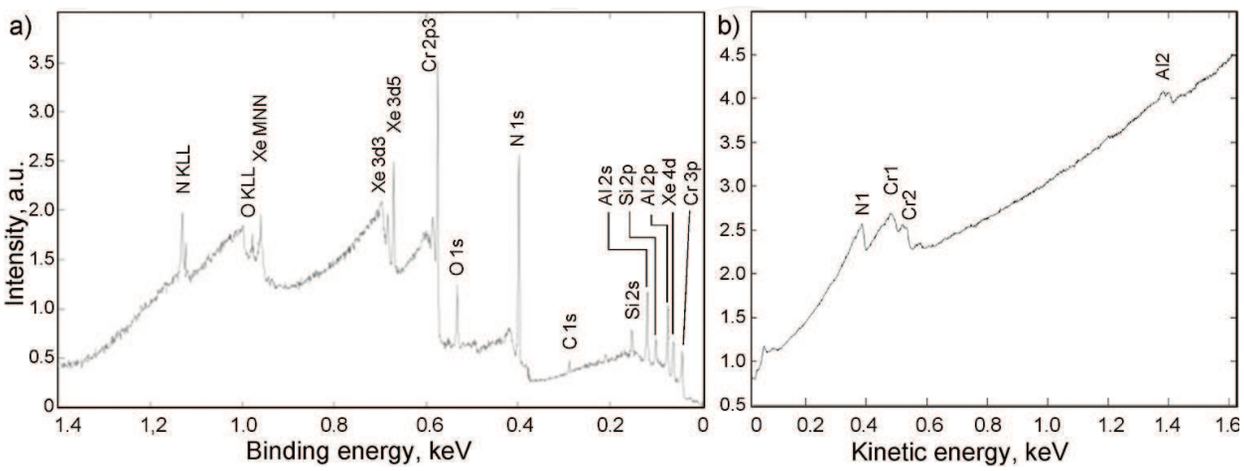

Figure 12. Spectrum of (a) XPS and (b) AES obtained from (Cr,Al,Si)N coating on tool ceramic-metallic material: (a) WS1 and (b) WS3; (a.u.)–arbitrary units.

a crater. The existence of the oxygen and carbon line should be associated with contamination. It was confirmed in chemical composition examinations with the AES method in areas created by etching with Xe+ ions that the chemical composition of the coatings is as assumed and a spectrum of Auger electrons obtained from the (Cr,Al,Si)N coatings has characteristic maximums corresponding to electron transitions for Cr LMM, Al KLL and N KLL.

It was also established based on fractographic tests carried out with a scanning electron microscope that the PVD and CVD coatings produced are deposited evenly and adhere tightly to the examined substrates (**Figure 13**). Particular layers in multilayer coating systems, i.e. Ti(C,N)+(Ti,Al)N, (Ti,Al)N+(Al,Cr)N, (Al,Cr)N+(Ti,Al)N, TiN+multiTiAlSiN+TiN, TiN+TiAlSiN+TiN, TiN+TiAlSiN+AlSiTiN, Ti(C,N)+Al_2O_3+TiN and Ti(C,N)+TiN, have a compact structure without delaminations and defects and tightly adhere to each other. The fractographic tests of sintered carbides and tool ceramics with coatings deposited by the PVD and CVD method do not reveal a fracture delamination along the separation area between the coating and the substrate, which also indicates good adhesion of the coatings produced to the substrate [60–62].

It was confirmed with X-ray diffraction methods and was described further in this chapter that multilayer Ti(C,N)+Al_2O_3+TiN and Ti(C,N)+TiN-type coatings fabricated with the CVD method in the coating-substrate interphase zone have a thin layer of a fine-grained TiC phase. Furthermore, a Ti(C,N) layer in CVD coatings is characterised by a structure changing in a gradient manner from a fine-grained structure near the substrate gradually transiting to a column structure. An Al_2O_3 layer exhibits a structure similar to a column structure. A top TiN layer in CVD coatings is very thin, thus preventing from determining its structure. A column structure of particular layers is also clearly visible in the case of two-layer Ti(C,N)+TiN and TiC+TiN coatings obtained on Si_3N_4 ceramics [60, 61].

It was also discovered by observing the fractures of PVD coatings that Ti(C,N) (1), (Al,Ti)N, (Ti,Al)N, Ti(C,N) (2), (Ti,Al)N+(Al,Cr)N, (Al,Cr)N+(Ti,Al)N coatings and (Al,Cr)N coatings fabricated by PVD possess a structure classified as the T zone according to Thornton's model [63]. Ti(B,N), (Ti,Zr)N coatings, though, feature a structure with thicker column grains (zone II

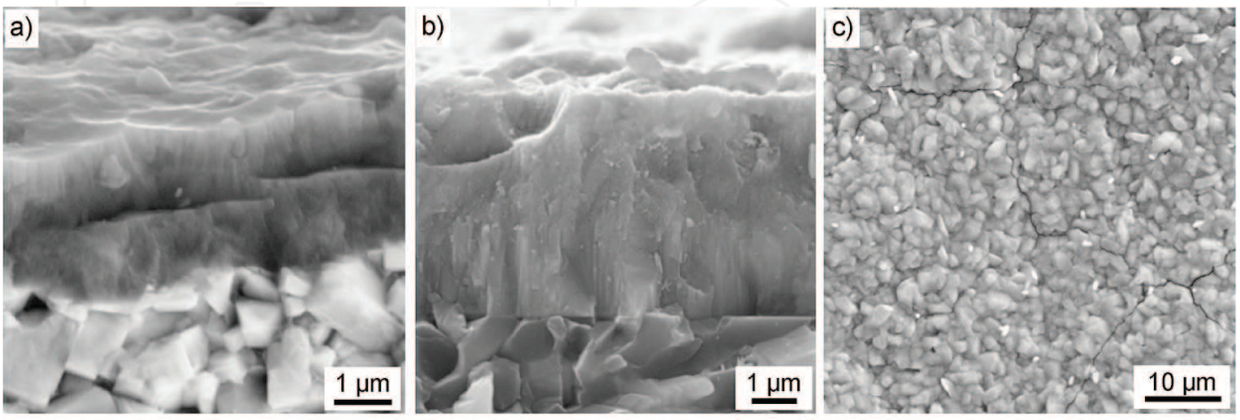

Figure 13. Fracture of the (a) Ti(C,N)+(Ti,Al)N coating deposited onto the sintered carbides substrate, (b) (Ti,Al)N+(Al,Cr)N coating deposited onto the sialon ceramics substrate and (c) surface topography of the Ti(C,N)+Al_2O_3+TiN coating deposited onto the cemented carbides substrate.

according to Thornton's model [63]). For a Ti(C,N)+(Ti,Al)N coating, the Ti(C,N) layer lying closer to the substrate and covering the two-third of the entire coating's thickness does not possess a column structure, but rather a fine-grained structure corresponding to the zone T according to Thornton's model. On the other hand, the (Ti,Al)N layer possesses a compact column structure classified as the transition zone between the zone T and zone II according to Thornton's model [63] (**Figure 13**).

The surface morphology of the coatings produced with the PVD technique is characterised by a high inhomogeneity because numerous droplet-shaped particles are present. The occurrence of such morphological defects is connected with the essence of the cathodic arc evaporation process. The size of such particles ranges between the tenths of a micrometer to a dozen or so micrometers. The presence of depressions was also discovered, which are formed, most probably, by solidified droplets being ejected after the end of the PVD process. For the coatings applied with the CVD method onto a substrate made of sintered carbides and tool ceramics, heterogeneity is seen in surface morphology related to the presence of multiple pores and networks of microcracks characteristic for such a process (**Figure 13c**). However, when an Al_2O_3 layer is situated on the substrate surface, or if this layer is in the under-the-surface zone (the top TiN layer is very thin), then the particles are needle-like or angularly shaped [60].

The observations of the surface morphology of (Cr,Al,Si)N and (Al,Ti,Si)N-type coatings on a substrate made of the investigated ceramic-metallic tool materials in a scanning electron microscope, in a microscope of atomic forces and in a confocal scanning microscope exhibit inhomogeneities connected with the occurrence of solidified microdroplets on the coating surface, characteristic for cathodic arc evaporation (**Figure 14**). Apart from droplets with a varied size of 1–5 μm, the agglomerates of particles with an elongated shape also exist, as well as depressions formed due to their ejection after finishing coating deposition. The examinations of chemical composition of microparticles, performed with an EDS spectrometer, indicate that Cr or Al prevails on their surface, which implies that these are metal droplets released from a disc, which solidify on the substrate surface.

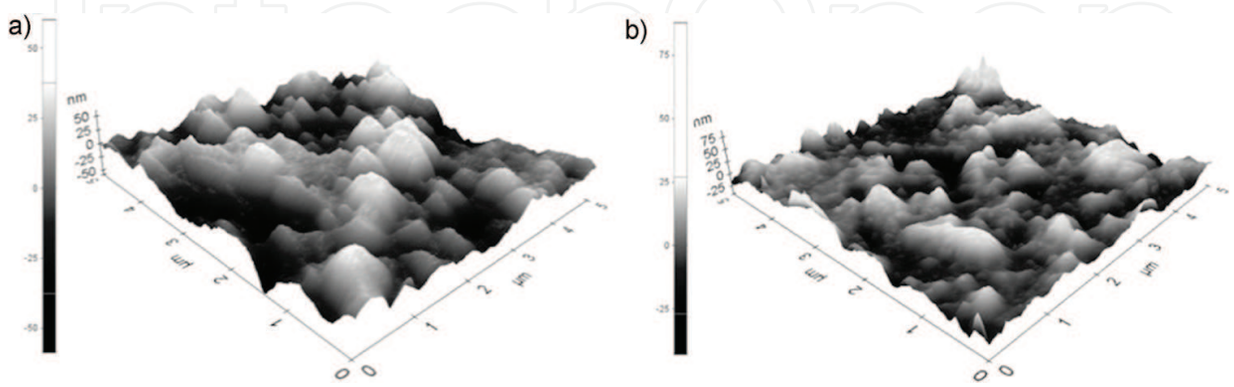

Figure 14. Surface topography of the following coatings (a) (Cr,Al,Si)N and (b) (Al,Ti,Si)N deposited onto ceramic-metallic tool material WS3; images produced using an atomic force microscope (AFM), 3D image.

It was found as a result of thin foils tests with an electron transmission microscope that coatings deposited in cathodic arc evaporation show a nanocrystalline structure. It was confirmed in a diffraction analysis that isomorphic phases exist with titanium nitride TiN in the case of TiN+multiTiAlSiN+TiN and Ti(B,N) coatings and the AlN phase with a hexagonal lattice in the case of an (Al,Ti)N coating. The presence of TiN and Al_2O_3 phases in TiN+Al_2O_3, TiN+Al_2O_3+TiN+Al_2O_3+TiN-type coatings was also confirmed, as assumed, in the investigations of coatings obtained by the CVD method. The Al_2O_3 layer structure with a rhombohedral lattice is characterised in its cross section by fine grains and grain size below 500 nm. A fine-crystalline structure of the TiN phase with a regular lattice is visible in the same cross section of thin foils between Al_2O_3 phase grains.

On the basis of investigations performed with an electron transmission microscope, (Cr,Al,Si)N and (Al,Ti,Si)N coatings were characterised, deposited onto a tool ceramic-metallic material, fabricated with the cathode arc evaporation (CAD) method with lateral arc rotating cathodes, composed of several layers and transition zones were investigated between the substrate as well as between the individual layers in the transmission mode and scanning-transmission mode, with BF and HAADF detectors (**Figure 15**). It was concluded based on the tests of thin foils from the cross section that they have a nanocrystalline and nanocomposite structure within the entire volume and they do not show discontinuities, cracks and porosity and have high homogeneity and a compact structure. The existence of several layers in nitride coatings was identified, both, based on Cr, Al and Si, as well as Al, Ti Si, exhibiting a varying thickness and chemical composition depending on the distance from the substrate. A layer deposited directly onto the near-the-core TiN layer shows a gradient character with a linearly decreasing concentration of Ti, accompanied by a heightening concentration of Al (**Figure 16a**) and the successive eight layers are characterised by a variable concentration of, respectively, Cr or Ti and Al (**Figure 16b**).

The HRTEM examinations of layers with a high concentration of Al prove the existence of nanograins with a differentiated orientation of planes showing the presence of long-range order typical in crystalline materials between which areas with a smaller degree of order

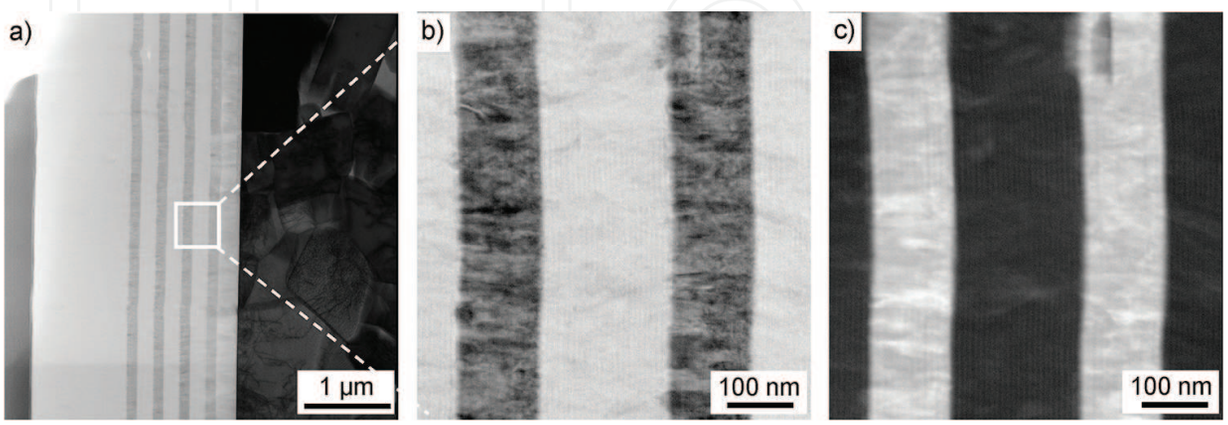

Figure 15. Structure of (Al,Ti,Si)N coatings; image in scanning-transmission mode with BF (a, b); HAADF (c) detector.

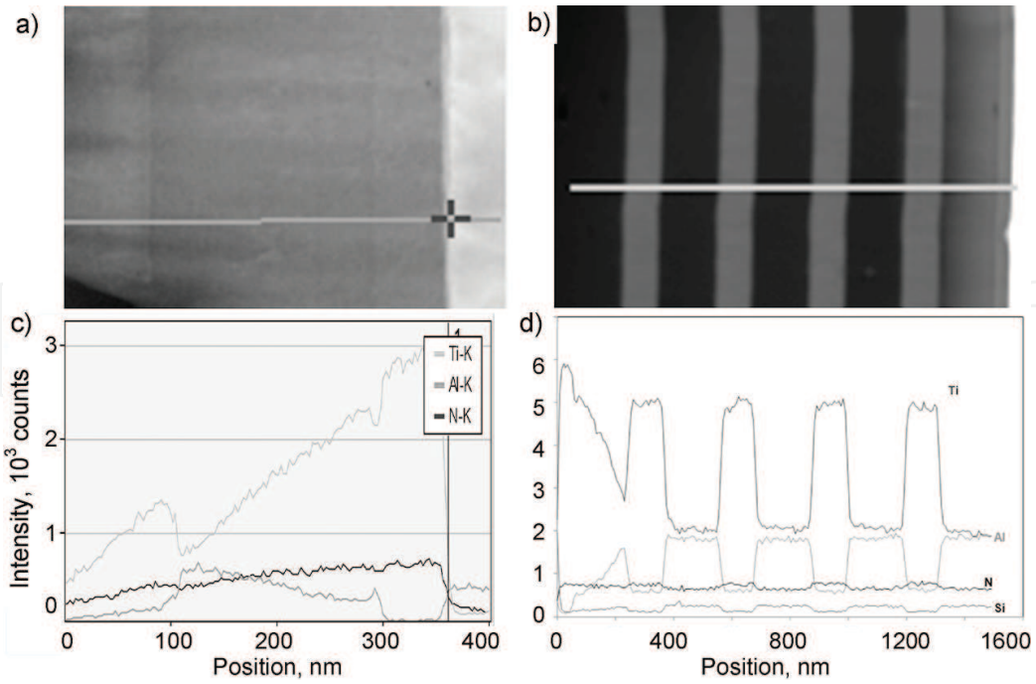

Figure 16. Profile analysis of variations in chemical composition made along the marked line using an energy dispersion spectrometer (a) and (b) of graded AlTiSiN layer (c) and (d) successive layers.

were identified. Structural observations and diffraction images using imaging in the HRTEM mode and the corresponding Fourier FFT transforms (**Figure 17**) confirm that the fabricated nitride coatings based on Al, Ti, Cr, Si exhibit a nanocrystalline and nanocomposite structure.

Profile and surface analyses of chemical composition variations performed with a high-resolution electron transmission microscope confirming the existence of transition layers between the substrate and coating and between individual layers with a varied concentration of Al and Ti may signify the existence of diffusive transition areas and thus contribute to the high adhesion of substrates produced with the cathodic arc evaporation method.

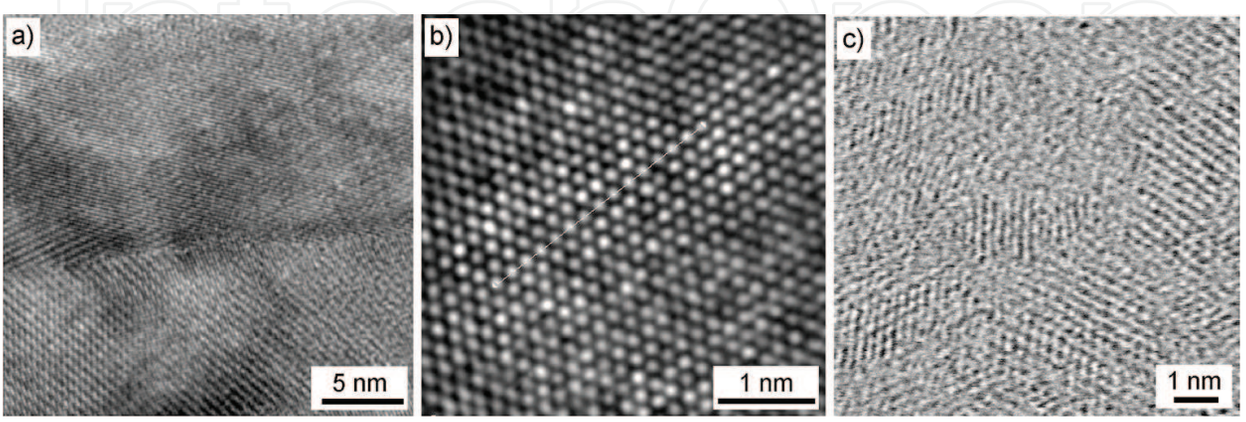

Figure 17. Coating structure (Al,Ti,Si)N (a) and (b) (3rd layer from substrate); image in HRTEM mode (c) (6th layer from substrate); image in scanning-transmission mode with BF detector.

http://dx.doi.org/10.5772/65400

5. Investigations into the properties of multicomponent coatings on the investigated sintered tool materials

The development directions of advanced tool materials, including sintered carbides, tool cermetals, tool ceramics and among others covered with anti-wear coatings, are pre-conditioning, to a high degree, improvements in the quality and efficiency of production. Enhanced operational properties are very frequently achieved for the commonly applied sintered tool materials by the deposition of coatings with PVD and CVD methods and not only simple monolayer or single-component coatings, but also complex multicomponent layers combining coatings with different properties, with each of them performing a relevant task and preferably continuous or graded coatings, with a gradual or continuous change of one or several components in the direction from the substrate to the outer surface, achieved in particular by PVD. The expected functional properties are achievable by selecting appropriately the substrate of indexable inserts and multicomponent coatings, also on sintered carbides and nitride and sialon ceramics. Their expected mechanical and operational properties can be ensured by forming the appropriate structure of coatings (presented in the previous chapter).

The thickness of the examined PVD coatings obtained on sintered carbides and nitride and sialon tool ceramics spans between 1.3 and 5.0 μm, while the thickness of CVD coatings between 2.8 and 10.0 μm. It was found as a consequence of the examinations performed that both PVD and CVD coatings on sintered carbides show a higher thickness than for substrates of the same type on a tool ceramics substrate. The exception are (Ti,Al)N and (Al,Cr)N coatings here, having a higher thickness on a sialon substrate. (Cr,Al,Si)N and (Al,Ti,Si)N coatings deposited onto ceramic-metallic tool materials are between 2.5 and 3 μm thick (**Table 3**).

The hardness of the sintered tool materials differs between 1826 HV for sintered carbides and 1850 HV for nitride ceramics and 2035 HV for sialon ceramics. The surface microhardness of the examined tool materials is greatly enhanced by depositing PVD and CVD coatings. The highest hardness is seen for multicomponent (Al,Ti)N coatings, TiN+multi(Ti,Al,Si)N+TiN multilayer coatings obtained by PVD, which accounts for nearly 100% growth in surface layer hardness in relation to the hardness of the uncoated material. The hardness of the examined coating systems is conditioning their abrasive wear, as seen most clearly for the TiN+Al_2O_3 coating—the hardest of the CVD coatings, thus contributing to the lower wear intensity of a tool cutting edge in cutting. To summarise, high abrasion resistance as well as good cutting properties of the tested tool ceramics with PVD and CVD coatings deposited are stemming from increased microhardness (**Table 3**).

It was pointed out in roughness examinations that the smallest value of the parameter R_a = 0.6 μm is seen for those surfaces of the examined sintered tool materials with no coating deposited. Following the deposition of PVD and CVD coatings onto the investigated substrates, the surface layer roughness increases and ranges R_a = 0.13–0.82 μm (**Table 3**). The increased surface roughness of the coatings deposited, in particular in the case of coatings obtained in a PVD process, should be associated with the character of the PVD cathodic arc evaporation process, as confirmed in morphological tests in a scanning electron microscope. The lowest value of the parameter R_a = 0.079 μm of ceramic-metallic tool materials is seen for the surface of the WS3

Process	Substrate	Coating	Thickness, μm	Roughness parameters R_a, μm	Microhardness, HV	Critical load Lc, N	Tool life, min
PVD	Cemented carbide	Ti(B,N)	1.8	0.29	2951	34	15
		(Ti,Zr)N	3.0	0.30	2842	40	13
		Ti(C,N) (1)	2.1	0.22	2871	49	13
		Ti(C,N)+(Ti,Al)N	2.8	0.31	3076	39	15
		Ti(C,N) (2)	2.1	0.50	3101	77	53
		(Al,Ti)N	2.5	0.18	3301	100	55
		(Ti,Al)N	3.5	0.39	3327	109	60
		(Al,Cr)N	3.8	0.28	2867	96	45
	Si_3N_4	TiN	0.8	0.34	2255	20	8
		TiN+multi(Ti,Al, Si)N+TiN	4.0	0.44	3592	22	10
		TiN+(Ti,Al,Si)N +TiN	2.0	0.45	2378	21	8
		TiN+(Ti,Al,Si)N +(Al,Si,Ti)N	2.5	0.32	2731	18	9
		Ti(B,N)	2.1	0.26	2898	12	8
		Ti(C,N)	2.1	0.34	3188	14	8
		(Ti,Zr)N	1.7	0.29	2798	30	12
		(Ti,Al)N	0.7	0.23	3408	42	14
	Sialon ceramics	(Ti,Al)N+(Al,Cr)N	4.0	0.45	3210	23	13
		(Al,Cr)N+(Ti,Al)N	3.9	0.44	2558	71	27
		Ti(C,N)+(Ti,Al)N	1.4	0.3	2786	36	6
		(Al,Ti)N	3.0	0.15	3600	112	72
		(Ti,Al)N	5.0	0.28	2961	21	9
		(Al,Cr)N	4.8	0.31	2230	53	50
		Ti(C,N) (2)	1.8	0.38	2843	26	9
		Ti(C,N) (1)	1.5	0.23	2872	25	5
		Ti(B,N)	1.3	0.25	2676	13	5
		(Ti,Zr)N	2.3	0.4	2916	21	5.5
	WS1	no coating	0	0.082	1621	–	14
	WS2		0	0.103	1497	–	11
	WS3		0	0.079	1711	–	16
	WS1	(Cr,Al,Si)N and nine layers	2.5–3	0.112	3388	116.2	78
	WS2		2.5–3	0.175	3250	100.4	59
	WS3		2.5–3	0.091	3472	124.6	82
	WS1		2.5–3	0.131	2856	104.3	62

Process	Substrate	Coating	Thickness, μm	Roughness parameters R_a, μm	Microhardness, HV	Critical load Lc, N	Tool life, min
	WS2	(Al,Ti,Si)N and nine layers	2.5–3	0.186	2252	97.2	50
	WS3		2.5–3	0.120	2908	112.3	68
	Cemented carbide	TiAlN	x	x	x	x	24
CVD	Cemented carbide	Ti(C,N) +Al_2O_3+TiN	8.4	0.63	2315	93	23
		Ti(C,N)+TiN	5.0	0.40	2443	110	27
	Si_3N_4	Ti(C,N)+TiN	4.2	0.15	2268	52	8
		Ti(C,N) +Al_2O_3+TiN	9.5	0.28	2050	27	8
		TiC+TiN	5.4	0.25	2020	67	10
		TiC+Ti(C,N) +Al_2O_3+TiN	7.8	0.27	3025	32	8
		TiN+ Al_2O_3	10.0	0.45	3320	83	16
		TiN+Al_2O_3+TiN	3.8	0.13	2487	48	15
		Al_2O_3+TiN (1)	2.6	0.25	2676	45	16
		Al_2O_3+TiN (2)	1.7	0.23	2775	27	14
		TiN+Al_2O_3+TiN+ Al_2O_3+TiN	4.5	0.6	2571	41	20
	Sialon ceramics	Ti(C,N) +Al_2O_3+TiN	7.0	0.82	2669	43	10
		Ti(C,N)+TiN	2.8	0.2	2746	72	15

x material used for comparison

Table 3. The results of the properties of sintered tool materials with the PVD and CVD coatings deposited.

material without a coating deposited. The roughness of WS1 and WS2 materials without coatings deposited is R_a = 0.082 and R_a = 0.103 μm, respectively. The results confirm that the deposition of (Cr,Al,Si)N and (Al,Ti,Si)N coatings applied onto substrates made of tool materials increases surface layer roughness and ranges R_a = 0.091–0.186 μm. The critical load value *L*c measuring the adhesion of PVD and CVD coatings to a substrate made of sintered carbides and nitride and sialon tool ceramics was determined in a scratch test. The critical load was determined as such corresponding to an increase in acoustic emission indicating the beginning of coating chipping and verification was made by measuring the friction force (F_t) of a diamond indenter and through metallographic observations in a light microscope connected to a measuring instrument. The critical load value *L*c (AE) for PVD coatings is between 13 and 131 N and for CVD coatings—between 15 and 110 N (**Table 3**). In the case of coatings deposited by the PVD method on sintered carbides, the best substrate adhesion is exhibited by (Ti,Al)N coatings, for which a critical load value *L*c = 109 N, whereas the weakest substrate adhesion is seen for the Ti (B,N) coatings, where *L*c = 34 N. The coatings deposited by the CVD method onto a substrate

made of sintered carbides show a high critical load of *L*c = 93 N for a Ti(C,N)+Al_2O_3+TiN coating and *L*c = 110 N for a Ti(C,N)+TiN coating [60, 61, 64]. The highest critical load of *L*c = 112 N for the PVD coatings obtained on nitride and sialon ceramics is shown by an (Al,Ti)N coating, whilst the lowest of *L*c = 13 N for a Ti(B,N) coating. Critical loads for the coatings obtained by CVD on nitride and sialon ceramics are between 27 and 83 N (**Table 3**). The highest critical load value of *L*c = 124.6 N and *L*c = 112.3 N, respectively, was identified for CrAlSiN and AlTiSiN coatings deposited onto a WS3-type substrate, as compared to WS1 and WS2 substrates. The similar dependencies were obtained for a WS1 and WS2 substrate (**Table 3**). The very good adhesion of PVD coatings, especially to a substrate made of sintered carbides and newly created ceramic-metallic tool materials and of CVD coatings to a substrate made of tool ceramics, stems from the fact that transition zones exist created at the substrate-coating boundary and at the boundary between two layers, as confirmed by tests with a transmission electron microscope and in a glow discharge spectrometer GDOES presented in the previous chapter. Coating damages formed as a result of adhesion tests with the scratch method were identified on the basis of observations in a scanning electron microscope. It was discovered subsequently to the observations that damages to PVD and CDV coatings are of the abrasive wear nature and are also characterised by a high number of single- or double-sided coating cracks at the scratch peripheries and by a delamination inside the scratch leading to coating delamination at the interface with the scratch. An increasing load during a scratch test is leading to intensified cracks at the scratch peripheries, causing a partial coating delamination. The periodical chipping of coatings also occurs (**Figure 18a**). CrAlSiN coatings deposited onto tool ceramic-metallic materials possess better substrate adhesion than AlTiSiN coatings. In the case of CrAlSiN coatings, the conformal fractures caused by stretching exist in the zone of first damages, changing into small flakings situated on the scratch bottom and peripheries and flakings and small arc chippings exist at the central zone of the scratch. Intensified conformal fractures, delamination and partial coating fragmentation take place on the scratch bottom as a load are increasing and single peripheral damages combine, thus forming local coating delamination

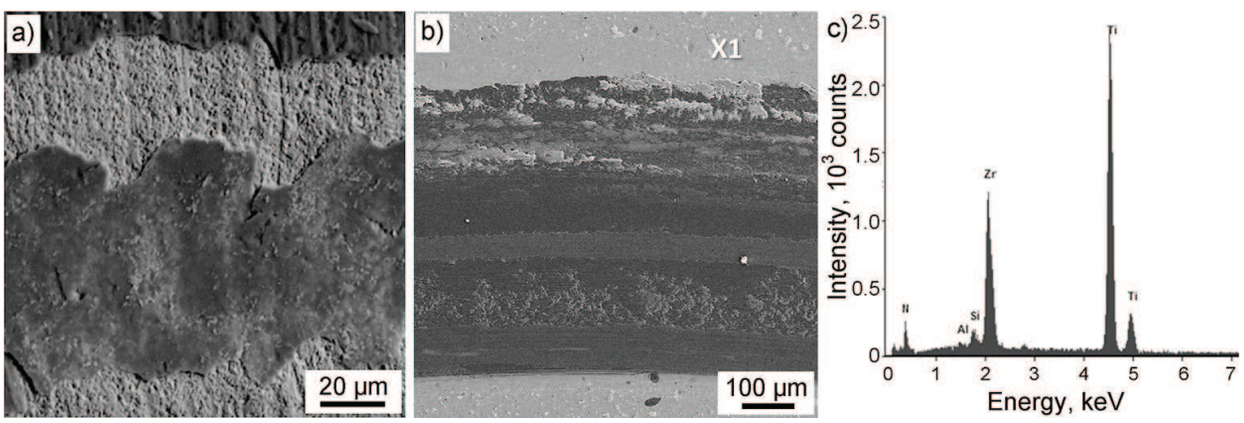

Figure 18. (a) Indenter mark for load above the critical load and the image of damages created as a result of scratch-test of Ti(B,N) coating deposited onto sintered carbides, (b) trace of tribological damage on the surface of (Ti,Zr)N coating deposited onto the substrate made of sialon ceramics and (c) diagrams of energy of backscatter X-ray radiation from the micro-area X1.

bands at most. The complete delamination of the CrAlSiN coating does not emerge in the final zone of the scratch with the maximum load on the penetrator.

An abrasion strength test with the pin-on-disc method was undertaken to determine fully the functional and operational characteristic of the investigated PVD and CVD coatings deposited onto a substrate of the selected sintered materials. The tests carried out show that the coatings deposited by CVD have worse tribological properties as compared to coatings deposited with the PVD technology. Coating damages to the substrate material zone occur in almost all the cases of the examined coatings. Damages to such coatings are accompanied by lost adhesion. The most frequent coating wear mechanisms are chippings and flaking as well as partial delamination (**Figure 18b** and **c**). An abrasive wear resistance test under dry slide friction conditions with the ball-on-plate method at room temperature was performed to determine the tribological properties of the examined coatings deposited on ceramic-metallic tool materials. It was stated by analysing the profiles of wear tracks formed after a tribological wear (after the distance of 500 m) that the maximum depths of wear are smaller than the thickness of a CrAlSiN, as well as an AlTiSiN layer, signifying that have not been fully worn. It can be concluded by analysing a field area of a wear track section of coatings and substrates that a CrAlSiN coating has the lowest wear index. An AlTiSiN coating has a larger field area of the wear track section and a higher wear index versus a CrAlSiN coating. The highest wear index is seen for a substrate made of WS3 tool materials.

The service life of the examined sintered tool materials was identified based on technological cutting tests. It was found as a result of cutting ability tests that the highest service life of $T = 72$ min was achieved for a cutting edge coated with an (Al,Ti)N coating, while the lowest life of $T = 5$ min on the same substrate is exhibited by Ti(B,N) and Ti(C,N) (1) coatings. The life of an uncoated cutting edge made of sialon ceramics was estimated at $T = 11$ min, which allows to confirm that (Al,Ti)N, (Al,Cr)N and Ti(C,N)+TiN coatings contribute to the enhanced life of a sialon cutting edge. A (Ti,Al)N coating has the greatest effect on the cutting edge life of $T = 60$ min for sintered carbide plates and slightly lower of $T = 55$ and 53 min, respectively, for (Al,Ti)N and Ti(C,N)(2) coatings. In the case of sintered carbides, all coatings increase the cutting edge life because the durability of an uncoated tool is $T = 2$ min, whilst the durability of plates with the lowest cutting ability with (Ti,Zr)N and Ti(C,N)(1) coatings is $T = 13$ min. A clear anti-wear impact of the presence of the combined Al_2O_3+TiN and TiN+Al_2O_3 coatings on the life of the inserts was found as a result of the grey cast iron rolling tests made with Si_3N_4 tool ceramics. A broad cutting edge durability range depending on the type of the applied coating was attained both for coated sintered carbides and coated tool nitride and sialon ceramics (**Table 3**). The hardness of ceramic-metallic tool materials as a substrate in a surface zone ranges between 1497 and 1711 HV0.1. After the deposition of CrAlSiN, AlTiSiN coatings on the examined WS1, WS2, WS3 ceramic-metallic tool materials, microhardness is growing substantially in the near-the-surface zone as compared to an uncoated substrate (**Table 3**). Dependence between substrate hardness and hardness of the deposited coating was not found. Where nanocrystalline, nanocomposite anti-wear coatings of CrAlSiN and AlTiSiN types are deposited onto tool materials, microhardness is growing substantially in the near-the-surface zone and—in connection with high substrate adhesion—contributes to lower wear intensity of cutting tools made from such materials, as was confirmed in the operational examinations. It was found as a result of metallographic observations in a scanning electron microscope for the

examined indexable inserts that the tools subjected to a cutting test indicate wear according to the abrasion and adhesion mechanism.

Additional information

The chapter was partially supported in the framework of the project 'NANOCOPOR—determining the importance of the effect of the one-dimensional nanostructural materials on the structure and properties of newly developed functional nanocomposite and nanoporous materials', funded by the DEC-2012/07/B/ST8/04070 of the Polish National Science Centre in the framework of the 'OPUS' competitions, headed by Prof. Leszek A. Dobrzański.

Author details

Leszek A. Dobrzański*, Daniel Pakuła, Klaudiusz Gołombek, Anna D. Dobrzańska-Danikiewicz and Marcin Staszuk

*Address all correspondence to: leszek.adam@gmail.com

Mechanical Engineering Faculty, Silesian University of Technology, Gliwice, Poland

References

[1] Dobrzański LA, Pakuła D, Staszuk M, Dobrzańska-Danikiewicz AD. Structure and properties of composite coatings on sintered carbide and nitride and sialon ceramics. Open Access Library. 2015;**5**:1–173 (in Polish).

[2] Dobrzański LA, Matula G. Powder metallurgy fundamentals and sintered materials. Open Access Library. 2012;**8**:1–156 (in Polish).

[3] Dobrzański LA. Engineering materials and materials design. Fundamentals of materials science and physical metallurgy. 2nd ed. Warsaw: WNT; 2006. 1600 p. (in Polish). ISBN 83-204-3249-9.

[4] Ruys A, Gingu O, Sima G, Maleksaeedi S. Powder processing of bulk components in manufacturing. In: Nee AYC, editor. Handbook of Manufacturing Engineering and Technology. London: Springer-Verlag; 2015. pp. 487–566. DOI: 10.1007/978-1-4471-4670-4_48.

[5] Gołombek K. Structure and properties of injection moulding tool materials with nanocrystalline coatings. Open Access Library. 2013;**1**:1–136 (in Polish).

[6] Dobrzański LA, Matula G. Powder injection molding: sinter-hardening. In: Colás R, Totten GE, editors. Encyclopedia of Iron, Steel and Their Alloys. Boca Raton: CRC Press, Taylor & Francis Group; 2016. 14 p. ISBN: 978-1-4665-1104-0.

[7] Matula G. Gradient surface layers from tool cermets formed pressurelessly and sintered. Open Access Library. 2012;**7**:1–144 (in Polish).

[8] German RM. Powder Metallurgy and Particulate Materials Processing. Princeton: Metal Powder Industries Federation; 2005. 528 p. ISBN 0-9762057-1-8.

[9] Kim S, Han SH, Park JK, Kim HE. Variation of WC grain shape with carbon content in the WC–Co alloys during liquid-phase sintering. Scripta Materialia. 2003;**48**:635–639. DOI: 10.1016/S1359-6462(02)00464-5.

[10] Holmberg K, Matthews A, editors. Coating Tribology. Properties, Mechanisms, Techniques and Applications in Surface Engineering. Tribology and Interface Engineering Series No. 56. Amsterdam: Elsevier; 2009. 576 p. ISBN 978-0-444-52750-9.

[11] Xiong J, Guo Z, Yang M, Wan W, Dong G. Tool life and wear of WC–TiC–Co ultrafine cemented carbide during dry cutting of AISI H13 steel. Ceramics International. 2013;**39**:337–346. DOI: 10.1016/j.ceramint.2012.06.031.

[12] Liu Y, Wang H, Long Z, Liaw PK, Yang J, Huang B. Microstructural evolution and mechanical behaviors of graded cemented carbides. Materials Science and Engineering: A. 2006;**426**:346–354. DOI: 10.1016/j.msea.2006.04.018.

[13] Zhang S. Handbook of Nanostructured Thin Films and Coatings. Boca Raton, London, New York: CRC Press, Taylor & Francis Group; 2010. 1232 p. ISBN 978-1420094350.

[14] Eriksson M, Radwan M, Shen Z. Spark plasma sintering of WC, cemented carbide and functional graded materials. International Journal of Refractory Metals and Hard Materials. 2013;**36**:31–37. DOI: 10.1016/j.ijrmhm.2012.03.007.

[15] German RM. Markets applications and financial aspects of global metal powder injection moulding (MIM) technologies. Metal Powder Report. 2012;**1**:18–26. DOI: 10.1016/S0026-0657(12)70051-6.

[16] Dobrzański LA, Matula G, Herranz G, Várez A, Levenfeld B, Torralba JM. Metal injection moulding of HS12-1-5-5 high-speed steel using a PW-HDPE based binder. Journal of Materials Processing Technology. 2006;**175**:173–178. DOI: 10.1016/j.jmatprotec.2005.04.033.

[17] Várez A, Levenfeld B, Torralba JM, Matula G, Dobrzański LA. Sintering in different atmospheres of T15 and M2 high speed steels produced by modified metal injection moulding process. Materials Science and Engineering: A. 2004;**366**:318–324. DOI: 10.1016/j.msea.2003.08.028.

[18] Matula G, Dobrzański LA, Várez A, Levenfeld B, Torralba JM. Comparison of structure and properties of the HS12-1-5-5 type high-speed steel fabricated using the pressureless forming and PIM methods. Journal of Materials Processing Technology. 2005;**162–163**:230–235. DOI: 10.1016/j.jmatprotec.2005.02.1.

[19] Dobrzański LA, Matula G, Várez A, Levenfeld B, Torralba JM. Structure and mechanical properties of HSS HS6-5-2- and HS12-1-5-5-type steel produced by modified powder

injection moulding process. Journal of Materials Processing Technology. 2004;**157–158**:658–668. DOI: 10.1016/j.jmatprotec.2004.07.1.

[20] Gołombek K, Matula G, Mikuła J, Dobrzański LA. Influence of binder composition on the properties of feedstock for cemented carbides. Archives of Materials Science and Engineering. 2011;**51**:116–124.

[21] Dobrzański LA, Matula G, Várez A, Levenfeld B, Torralba JM. Fabrication methods and heat treatment conditions effect on tribological properties of high speed steels. Journal of Materials Processing Technology. 2004;**157–158**:324–330. DOI: 10.1016/j.jmatprotec.2004.09.051

[22] Mikuła J, Matula G, Gołombek K, Dobrzański LA. Sintered composite gradient tool materials. Archives of Materials Science and Engineering. 2008;**32**:25–28.

[23] Matula G, Dobrzański LA, Ambroziak M. Simulation of powder injection moulding conditions using cadmould program. Journal of Achievements in Materials and Manufacturing Engineering. 2012;**55**:556–560.

[24] Matula G, Dobrzański LA, Várez A, Levenfeld B. Development of a feedstock formulation based on PP for MIM of carbides reinforced M2. Journal of Achievements in Materials and Manufacturing Engineering. 2008;**27**:195–198.

[25] Matula G, Dobrzański LA, Herranz G, Várez A, Levenfeld B, Torralba JM. Structure and properties of HS6-5-2 type HSS manufactured by different P/M methods. Journal of Achievements in Materials and Manufacturing Engineering. 2007;**24**:71–74.

[26] Dobrzański LA, Gołombek K, Lukaszkowicz K. Physical vapor deposition in manufacturing. In: Nee AYC, editor. Handbook of Manufacturing Engineering and Technology. London: Springer-Verlag; 2015. pp. 2719–2754. DOI: 10.1007/978-1-4471-4670-4_29.

[27] Dobrzański LA, Dobrzańska-Danikiewicz AD. Engineering materials surface treatment. Open Access Library. 2011;**5**:1–480 (in Polish).

[28] Dobrzański LA, Pakuła D, Staszuk M. Chemical vapor deposition in manufacturing. In: Nee AYC, editor. Handbook of Manufacturing Engineering and Technology. London: Springer-Verlag; 2015. pp. 2755–2803. DOI: 10.1007/978-1-4471-4670-4_30.

[29] Lukaszkowicz K, Dobrzański LA, Sondor J. Microstructure, mechanical properties and corrosion resistance of nanocomposite coatings deposited by PVD technology. In: Reddy BSR, editor. Advances in Diverse Industrial Applications of Nanocomposites. Rijeka: InTech; 2011. pp. 1–16. DOI: 10.5772/14117.

[30] Staszuk M, Dobrzański LA, Tański T, Kwaśny W, Musztyfaga-Staszuk M. The effect of PVD and CVD coating structures on the durability of sintered cutting edges. Archives of Metallurgy and Materials. 2014;**59**:269–274. DOI: 10.2478/amm-2014-0044.

[31] Dobrzański LA, et al. Investigations of Structure and Properties of Newly Created Porous Biomimetic Materials Fabricated by Selective Laser Sintering, BIOLASIN. Project UMO-2013/08/M/ST8/00818. Gliwice: Silesian University of Technology; 2013–2016.

[32] Dobrzański LA. Applications of newly developed nanostructural and microporous materials in biomedical, tissue and mechanical engineering. Archives of Materials Science and Engineering. 2015;**76**:53–114.

[33] Dobrzański LA, Dobrzańska-Danikiewicz AD, Gaweł TG, Achtelik-Franczak A. Selective laser sintering and melting of pristine titanium and titanium Ti6Al4V alloy powders and selection of chemical environment for etching of such materials. Archives of Metallurgy and Materials. 2015;**60**:2039–2045. DOI: 10.1515/amm-2015-0346.

[34] Dobrzański LA, Dobrzańska-Danikiewicz AD, Malara P, Gaweł TG, Dobrzański LB, Achtelik-Franczak A. Fabrication of scaffolds from Ti6Al4V powders using the computer aided laser method. Archives of Metallurgy and Materials. 2015;**60**:1065–1070. DOI: 10.1515/amm-2015-0260.

[35] Kremzer M, Dobrzański LA, Dziekońska M, Macek M. Atomic layer deposition of TiO_2 onto porous biomaterials. Archives of Materials Science and Engineering. 2015;**75**:63–69.

[36] Dobrzański LA, Dobrzańska-Danikiewicz AD, Szindler M, Achtelik-Franczak A, Pakieła W. Atomic layer deposition of TiO_2 onto porous biomaterials. Archives of Materials Science and Engineering. 2015;**75**:5–11.

[37] Dobrzański LA, Dobrzańska-Danikiewicz AD, Achtelik-Franczak A, Dobrzański LB. Comparative analysis of mechanical properties of scaffolds sintered from Ti and Ti6Al4V powders. Archives of Materials Science and Engineering. 2015;**73**:69–81.

[38] Dobrzański LA, Dobrzańska-Danikiewicz AD, Gaweł TG. Ti6Al4V porous elements coated by polymeric surface layer for biomedical applications. Journal of Achievements in Materials and Manufacturing Engineering. 2015;**71**:53–59.

[39] Lukaszkowicz K, Dobrzański LA, Kokot G, Ostachowski P. Characterization and properties of PVD coatings applied to extrusion dies. Vacuum. 2012;**86**:2082–2088. DOI: 10.1016/j.vacuum.2012.04.025.

[40] Dobrzański LA, Staszuk M, Gołombek K, Śliwa A, Pancielejko M. Structure and properties PVD and CVD coatings deposited onto edges of sintered cutting tools. Archives of Metallurgy and Materials. 2010;**55**:187–193.

[41] Dobrzański LA, Żukowska LW, Mikuła J, Gołombek K, Pakuła D, Pancielejko M. Structure and mechanical properties of gradient PVD coatings. Journal of Materials Processing Technology. 2008;**201**:310–314. DOI: 10.1016/j.jmatprotec.2007.11.283.

[42] Dobrzański LA, Pakuła D, Kříž A, Soković M, Kopač J. Tribological properties of the PVD and CVD coatings deposited onto the nitride tool ceramics. Journal of Materials Processing Technology. 2006;**175**:179–185. DOI: 10.1016/j.jmatprotec.2005.04.032.

[43] Dobrzański LA, Gołombek K, Hajduczek E. Structure of the nanocrystalline coatings obtained on the CAE process on the sintered tool materials. Journal of Materials Processing Technology. 2006;**175**:157–162. DOI: 10.1016/j.jmatprotec.2005.04.008.

[44] Dobrzański LA, Mikuła J. The structure and functional properties of PVD and CVD coated Al_2O_3 + ZrO_2 oxide tool ceramics. Journal of Materials Processing Technology. 2005;**167**:438–446. DOI: 10.1016/j.jmatprotec.2005.05.034.

[45] Soković M, Mikuła J, Dobrzański LA, Kopač J, Kosec L, Panjan P, Madejski J, Piech A. Cutting properties of the Al_2O_3 + $SiC_{(w)}$ based tool ceramic reinforced with the PVD and CVD wear resistant coatings. Journal of Materials Processing Technology. 2005;**164–165**:924–929. DOI: 10.1016/j.jmatprotec.2005.02.071.

[46] Dobrzański LA, Pakuła D. Comparison of the structure and properties of the PVD and CVD coatings deposited on nitride tool ceramics. Journal of Materials Processing Technology. 2005;**164–165**:832–842. DOI: 10.1016/j.jmatprotec.2005.02.094.

[47] Dobrzański LA, Mikuła J. Structure and properties of PVD and CVD coated Al_2O_3 + TiC mixed oxide tool ceramics for dry on high speed cutting processes. Journal of Materials Processing Technology. 2005;**164–165**:822–831. DOI: 10.1016/j.jmatprotec.2005.02.089.

[48] Dobrzański LA, Gołombek K. Structure and properties of the cutting tools made from cemented carbides and cermets with the TiN+mono-, gradient- or multi(Ti,Al,Si)N+TiN nanocrystalline coatings. Journal of Materials Processing Technology. 2005;**164–165**:805–815. DOI: 10.1016/j.jmatprotec.2005.02.072.

[49] Pakuła D, Dobrzański LA, Gołombek K, Pancielejko M, Kříž A. Structure and properties of the Si_3N_4 nitride ceramics with hard wear resistant coatings. Journal of Materials Processing Technology. 2004;**157–158**:388–393. DOI: 10.1016/j.jmatprotec.2004.09.060.

[50] Gołombek K, Dobrzański LA, Soković M. Properties of the wear resistant coatings deposited on the cemented carbides substrates in the cathodic arc evaporation process. Journal of Materials Processing Technology. 2004;**157–158**:341–347. DOI: 10.1016/j.jmatprotec.2004.09.053.

[51] Dobrzański LA, Pakuła D, Hajduczek E. Structure and properties of the multicomponent TiAlSiN coatings obtained in the PVD process in the nitride tool ceramics. Journal of Materials Processing Technology. 2004;**157–158**:331–340. DOI: 10.1016/j.jmatprotec.2004.09.052.

[52] Dobrzański LA, Dobrzańska-Danikiewicz AD. Foresight of the surface technology. In: Nee AYC, editor. Handbook of Manufacturing Engineering and Technology. London: Springer-Verlag; 2015. pp. 2597–2637. DOI: 10.1007/978-1-4471-4670-4_26

[53] Dobrzańska-Danikiewicz AD. Foresight of material surface engineering as a tool building a knowledge-based economy. Materials Science Forum. 2012;**706–709**:2511–2516. DOI: 10.4028/www.scientific.net/MSF.706-709.2511.

[54] Dobrzańska-Danikiewicz AD. The book of critical technologies of surface and properties formation of engineering materials. Open Access Library. 2012;**6**:1–823 (in Polish).

[55] Dobrzańska-Danikiewicz AD. The acceptation of the production orders for the realisation in the manufacturing assembly systems. Journal of Materials Processing Technology. 2006;**175:**123–132. DOI: 10.1016/j.jmatprotec.2005.04.001.

[56] Krenczyk D, Dobrzańska-Danikiewicz A. The deadlock protection method used in the production system. Journal of Materials Processing Technology 2005;**164–165**:123–132. DOI: 10.1016/j.jmatprotec.2005.02.056

[57] Gołombek K. Structure and properties of the cemented carbides and tool cermets covered of wear resistant coatings in the PVD process [Ph.D. Thesis]. Gliwice, Poland: Silesian University of Technology; 2001 (in Polish).

[58] Adamiak M. Structure and properties of the TiN and Ti(C,N) PVD coatings deposited on high speed steels [Ph.D. Thesis]. Gliwice, Poland: Silesian University of Technology; 1997 (in Polish).

[59] Lukaszkowicz K. Forming the structure and properties of hybrid coatings on reversible rotating extrusion dies. Journal of Achievements in Materials and Manufacturing Engineering. 2012;**55**:159–224.

[60] Pakuła D. Structure and properties of the multilayers PVD and CVD wear resisted coatings on the Si_3N_4 tool nitride ceramics [Ph.D. Thesis]. Gliwice, Poland: Silesian University of Technology; 2003 (in Polish).

[61] Staszuk M. Structure and properties of the gradient PVD and CVD coatings on the sialons and sintered carbides [Ph.D. Thesis]. Gliwice, Poland: Silesian University of Technology; 2009 (in Polish).

[62] Pakuła D. Forming of the surface structure and properties of tool's ceramic inserts with improved abrasion resistance. Archives of Materials Science and Engineering. 2013;**62**:55–96.

[63] Thornton JA. The microstructure of sputter-deposited coatings. Journal of Vacuum Science and Technology A. 1986;**4**:3059–3065. DOI: 10.1116/1.573628.

[64] Pakuła D, Staszuk M, Dobrzański LA. Investigations of the structure and properties of PVD coatings deposited onto sintered tool materials. Archives of Materials Science and Engineering. 2012;**58**:219–226.

IntechOpen